

Single Particle ICP-MS: Advances toward routine analysis of nanomaterials

Manuel D. Montaña¹ · John W. Olesik² · Angela G. Barber³ · Katie Challis³ · James F. Ranville³

Received: 17 February 2016 / Revised: 22 May 2016 / Accepted: 31 May 2016 / Published online: 23 June 2016
© Springer-Verlag Berlin Heidelberg 2016

Abstract From its early beginnings in characterizing aerosol particles to its recent applications for investigating natural waters and waste streams, single particle inductively coupled plasma-mass spectrometry (spICP-MS) has proven to be a powerful technique for the detection and characterization of aqueous dispersions of metal-containing nanomaterials. Combining the high-throughput of an ensemble technique with the specificity of a single particle counting technique and the elemental specificity of ICP-MS, spICP-MS is capable of rapidly providing researchers with information pertaining to size, size distribution, particle number concentration, and major elemental composition with minimal sample perturbation. Recently, advances in data acquisition, signal processing, and the implementation of alternative mass analyzers (e.g., time-of-flight) has resulted in a wider breadth of particle analyses and made significant progress toward overcoming many of the challenges in the quantitative analysis of nanoparticles. This review provides an overview of spICP-MS development from a niche technique to application for routine analysis, a discussion of the key issues for quantitative analysis, and

examples of its further advancement for analysis of increasingly complex environmental and biological samples.

Keywords Single particle ICP-MS · ICP-TOF-MS · Engineered nanoparticles · Environmental analysis · Core-shell nanoparticles · FFF-ICP-MS

Need for advanced metrology and historical context

Nanotechnology represents a 21st century enabling technology which, through the control of matter between the scale of molecular dimensions to a few tens of nanometers, possesses the potential to make great advances in materials engineering. The continued development of nanotechnology requires increasingly sophisticated nanometrology capable of providing accurate and robust quantitation and characterization of nanoparticles (NPs) and nanoscale features. Instrumentation and standardized methods are well developed for examining nano-scale features on surfaces and have been commercially available for decades. Among the numerous approaches, key examples are electron and atomic force microscopy, the results of which can be rigorously traceable back to reference standards. The condition is somewhat different for nano-scale dispersed materials (i.e., NPs) where complications arise due to (1) the need to make measurements in potentially complex matrices, (2) obtain information on multiple measurands (e.g., size distribution, chemical composition, shape, etc.), and (3) account for the fact that NP characteristics are matrix-dependent and dynamic, responding to various processes such as aggregation, dissolution, and surface modification. Well-developed and validated NP characterization techniques such as light-scattering (dynamic and static) are challenged when samples contain background NPs that interfere with the measurement of the properties of interest for the

Published in the topical collection *Single-particle-ICP-MS Advances* with guest editors Antonio R. Montoro Bustos and Michael R. Winchester.

✉ Manuel D. Montaña
manuel.montano@duke.edu

- ¹ Department of Civil and Environmental Engineering, Duke University, Center for Environmental Implications of Nanotechnology, Durham, NC 27708, USA
- ² School of Earth Sciences, Ohio State University, 125 S. Oval Mall, 275 Mendenhall Lab, Columbus, OH 43210, USA
- ³ Department of Chemistry and Geochemistry, Colorado School of Mines, 1012 14th Street, Golden, CO 80401, USA

target NPs (e.g., particle size distribution). Even in simple matrices, some methods such as light scattering are simply unsuitable for measuring NP concentrations.

In response to these challenges, the sensitivity and the elemental specificity of inductively coupled plasma-mass spectrometry (ICP-MS) has been adapted to the analysis of NPs on a particle-by-particle basis, a technique commonly referred to in the literature as single particle ICP-MS (SP-ICPMS or spICP-MS depending on the author). This method is based on the generation of discrete pulses of ions that arise from single particles sequentially introduced into the ICP-MS. The recent explosive growth of this method for aqueous dispersions of NPs is in part a result of new developments in commercial ICP-MS hardware and software. Both the response of the instrument manufacturers and the increasing adoption of the method by the scientific community have been largely driven by concerns for the environmental health and safety of NPs as a consequence of their growing use in nanotechnology. The applicability of single particle ICP-MS to nanomaterials synthesis and manufacturing is obvious, but is as of yet largely unexplored. Growth in the use of single particle ICP-MS for measurement of aqueous dispersions of colloids and NPs is clearly demonstrated both by the fact that a bibliographic search found more than 45 relevant publications since the beginning of 2015, compared with the single seminal paper by Degueldre and Favarger in 2003 [1], and by the publication of this ABC themed issue.

Prior to describing spICP-MS methodology and discussing recent work, it is illustrative to examine its path of development and the driving forces behind it. For over 150 years, the fields of colloid chemistry and materials science have demonstrated a need for analysis tools applicable to inorganic NPs. In actuality, it is arguably the recognition of the importance of fine particles and colloids in the environment that led to the initial developments in single particle analysis by element-specific methods. While key needs arose regarding colloid and particle characterization in soil science [2, 3] and oceanography [4–6], atmospheric sciences was the most direct driver for the development of techniques for individual particle (i.e., aerosol) analysis. Earlier methods applied to aerosols utilized trapping particles on filters, impactors, or electrostatic precipitators [7]. However, an early report by Edwards [8], demonstrated that AgI particles, used for cloud seeding, could be directly measured in air by atomic adsorption spectroscopy (AAS). Although the concentration of Ag was determined, this was not a single particle method and no information on the nature of the AgI particles was obtained. Particle size and concentration analysis by a somewhat similar approach was the topic of Crider's [9] work on the development of an aerosol analyzer that detected the spectrochemical emission of individual particles as they passed through a hydrogen-

acetylene flame, with the purpose of determining the particle number concentration. A 1974 US Patent [10] granted to Sartorius-Membranfilter (GmbH) described the development of an instrument where particles are introduced "singly in succession into the evaporating zone of an atomic absorption spectrometer...said zone being small enough to be completely filled by a single evaporated particle."

These works are among the first to exploit analysis of the frequency of "flashes," observed by an element-specific measurement, to potentially determine particle number concentrations. The introduction of inductively coupled plasma-atomic emission spectroscopy [11, 12] allowed for the analysis of refractory elements that were not observable by flame AA. The work of Kawaguchi et al. [11] utilized generation of monodisperse aerosols containing the dissolved element of interest. Further work from this group, in which aerosols containing Zn and Pb were examined, introduced the use of ICP-MS [13–16] to improve detection limits. It should be noted that throughout the 1970s and 1980s, numerous other researchers had initiated work that led to the method of real-time single particle mass spectrometry (RTSPMS), also called continuous aerosol mass spectrometry [17].

Recent decades of research have demonstrated the possibility that low solubility contaminants could be transported through groundwater as a result of their adsorption to mobile colloids [18]. This concern stimulated the initial adoption of spICP-MS analysis to aqueous dispersions of colloids and NPs. Of particular concern was the potential for transport of radionuclides in groundwaters associated with underground nuclear weapons testing [19] and proposed nuclear waste repositories [20]. The application of spICP-MS as a possible means to characterize these materials was first proposed by McCarthy and Degueldre, who cite the prior aerosol literature as well as a personal communication with B. Wernli [21]. This led a decade later to a series of key papers by Degueldre et al. [1, 22–25] that established the basic methodology of the spICP-MS technique as we know it now. It was some years between the publication of these papers and the renewed interest in spICP-MS as a stand-alone method for characterizing NPs [26] and as a powerful means to further characterize size fractionated NPs [27]. The continual and rapid increase in the use of nanomaterials and the environmental health and safety concerns regarding implementation of nanotechnology have contributed to the significant increase in interest in this approach to complement other available techniques [28, 29]. It is not the purpose of this article to review all the work performed since the publication of a 2014 review article by Laborda et al. [30]. Rather it is the rapid adoption of this technique, with the goal of making single particle analysis routine, which leads us to review recent work that has identified and, in some case, addressed the challenges as well as the opportunities of the method.

Considerations for the application of single particle ICP-MS for routine nanomaterial analysis

Works of Kawaguchi [11], and of Degueldre [1, 22–24], demonstrated the feasibility of using ICP-MS for the analysis of colloids, but more work was needed to develop a technique that could provide additional meaningful information about the particles analyzed. In order to characterize and quantify unknown particles samples, several aspects of signal acquisition, data processing, and calibration must be addressed. The complexity of biological and environmental matrices also requires robust data processing to quantify particle signals amidst a high background of dissolved analyte and molecular interferences. The following discussion addresses the components of single particle analysis, and the many improvements in data acquisition and automated analysis that have been made in recent years that may lead to the potential of making single particle analysis possible in any lab equipped with an ICP-MS.

Calibration and optimization

There are a number of approaches to quantitatively determine nanoparticle size and number concentration by single particle ICP-MS. Though most ICP-MS instruments are capable of single particle analysis, steps need to be taken prior to analysis to ensure accurate results. Most importantly, it is generally necessary to account for the incomplete transport of nanoparticles in suspensions and elements in solution from the nebulizer into the plasma, and the implications this holds for equating ion signal to analyte mass accurately equating the number of detected NP events to the original NP number concentration in suspension. The following approaches have different requirements of what information is needed for calibration.

Size calibration by nanoparticle standards and microdroplets

The most intuitive way to size NPs in an unknown sample via spICP-MS is to generate a calibration curve of signal intensity versus particle diameter (i.e., mass). This utilizes different sizes of standard NPs, containing the same element as the target analyte nanoparticle. If the geometry and density is also the same for both standard and target nanoparticle, a direct relationship between particle size and instrument response can be generated [26, 31]. Recently, Lee and Chan [32], and Olesik and Gray [31] have demonstrated the potential for non-linearity in the calibration curves as a result of incomplete vaporization of larger NPs. This incomplete vaporization depends on the particle density, atomic weight, and melting point, which impact the particle's heat of vaporization. Though the use of standard NPs is arguably the most

straightforward approach for calibration and subject to fewer analysis variables, the relative scarcity of monodisperse, well-characterized nanoparticle standards for most elements limits the type of particles that can be analyzed using this approach.

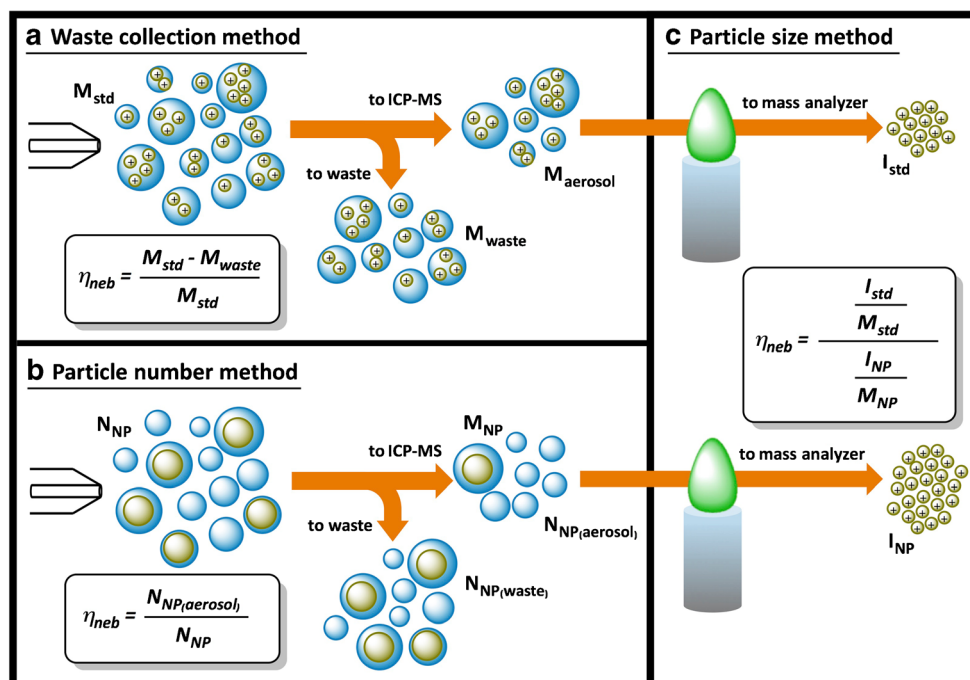
In the absence of particle standards, microdroplet generators (MDG) have garnered significant interest as an alternative to conventional nebulizers and spray chambers. Microdroplet generators are capable of introducing individual, monodisperse droplet into the plasma with 100 % efficiency, each of which produce a signal pulse that is identical to that produced by a particle of equivalent analyte element mass. In principal, if the solution concentration and droplet size are accurately known, the analyte mass entering the plasma is known and can be used to compute the relationship between analyte mass and instrument response (counts/element mass) for any element [33, 34]. Recently, these MDGs have been applied to the analysis of nanomaterials by ICP-OES [35], ICP-MS [36], and ICP-TOFMS [37]. The signal generated from droplets containing analyte elements show considerable precision, with relative standard deviations below 5 % in most cases. The signal generated from monodisperse droplets is dependent on their size, but the time integrated average signal is comparable to that of conventional nebulization [36, 38] at the typically used droplet generation frequency. The continued development of this technology may lead to more accurate and precise spICP-MS analysis than is afforded by conventional sample introduction systems.

Size calibration using standard solutions and analyte transport efficiency

The more common calibration route for single particle size analysis relates the intensity of dissolved standards, generated by conventional nebulization, to the mass of the particle (Fig. 1). In order to obtain this relationship, an experimental approach through which a dissolved calibration curve can be used to determine the mass of analyte generated from a particle event is required. There are several approaches to obtaining this relationship. These have been described in detail in NIST Special Publication 1200-21 (Murphy et al, 2015).

The most common sample introduction system for ICP-MS is a pneumatic nebulizer that nebulizes the liquid sample into a spray chamber at typical flow rates of 0.1–1.0 mL/min. The number of droplets that reach the plasma represent a small (<20 %) fraction of the total volume of sample introduced; this fraction is termed the transport efficiency (η_{neb}). This term is significant within the context of calibration using dissolved samples as the signal generated represents only a fraction of the volume delivered by the peristaltic pump. Thus, the mass of dissolved isotope that generates a given signal is less than what would be predicted from sample concentration and sample flow rate to the nebulizer. In contrast, changes in transport efficiency affect the number of nanoparticle signal pulses per

Fig. 1 Methods for determining transport efficiency for single particle ICP-MS



second, but not the signal produced by each nanoparticle that does enter the plasma.

Pace et al. [39] describe a method of sizing analysis using analysis of a nanoparticle standard to generate a mass flux curve from a dissolved standards calibration. In this approach, the concentration calibration curve is used to generate the element mass delivery to the plasma by normalization to a known measurement time. The mass flux term is given in Equation 1.

$$W = C_{STD} * \eta_{neb} * Q_{sample} * t_{dwell} \quad (1)$$

where

W	mass delivered per dwell time
C_{STD}	mass concentration (mass * volume ⁻¹)
η_{neb}	nebulization (transport) efficiency
Q_{sample}	sample flow rate (volume * time ⁻¹)
t_{dwell}	dwell time (time)

By relating the measured intensity to the mass delivered by the dissolved standards, the mass of the analyte in the NP can be determined. Concentration, sample flow rate and dwell time are all user-defined, but the transport efficiency must be determined experimentally, unless it is known to be 100 %. The three methods for determining this value, shown in Fig. 1 were examined by Pace et al. [39].

Method 1 for determining the transport efficiency is termed the waste collection method. The method that employs the simplest measurement, but least accurate results, is an indirect measurement of the transport efficiency via waste collection

(Fig. 1A). Knowledge of the sample flow rate and waste collection time allows the user to calculate the total volume of sample that entered the plasma by subtracting the volume of waste collected from the volume of solution delivered to the nebulizer. The ratio of this difference to the total delivered to the nebulizer gives the transport efficiency. This method should not be used as it is subject to a number of uncertainties (chief among them being evaporation), including that which arises from the need to subtract two large numbers (volume delivered to nebulizer and volume to waste) when the transport efficiency is low (typical when the sample uptake rate is greater than about 0.1 mL/min), and the inconsistency in waste drainage from the spray chamber [40, 41]. Recently, an attempt to reduce these sources of inaccuracy by measuring the ICP-MS signal from the sample and from the collected waste has been described [42] but not yet widely tested. The aerosol exiting the spray chamber can be measured directly by a filter collection method [41], but it is quite time-consuming and can be challenging to obtain RSDs better than 20 %.

Method 2 uses particle number concentration to determine the transport efficiency. The underlying assumption in spICP-MS is that each nanoparticle that enters the plasma will produce an ICP-MS signal pulse. If a standard particle suspension of known particle number concentration is delivered to the nebulizer at a known sample uptake rate, the number of nanoparticles delivered to the nebulizer per second can be calculated. The number of ICP-MS signal peaks per second is equal to the number of NPs that entered the plasma per second. The ratio of the measured number of signal particle peaks per second to the number of nanoparticles delivered to the

nebulizer per second is the transport efficiency. (Fig. 1b) as computed by Equation 2.

$$\eta_{neb} = \frac{N_{NP \text{ aerosol}}}{N_{NP}} \quad (2)$$

where

η_{neb}	nebulization (transport) efficiency
$N_{NP \text{ aerosol}}$	number of NPs reaching the plasma
N_{NP}	number of NPs delivered to the nebulizer

If the standard particle number concentration is not known, it can be estimated if the mass concentration, particle density, size, and shape are known (the same parameters as needed for the particle size method described below). Conceptually, this is the most direct means of establishing the transport efficiency, requiring none of the assumptions used in method 3. However, it can be experimentally challenging to implement. This approach requires that the actual NP number concentration at the time of analysis must be the same as the reported number value or, if computed, the mass concentration value must be as the stated value. If this assumption is not valid, the mass concentration of the standard should be verified at the time of analysis or the number concentrations must be determined by an independent method. Colloidal suspensions are inherently dynamic, where their stability is a balance of the electrostatic repulsion and the attractive van der Waals forces between particles [43, 44]. Collisions between particles may result in aggregation and settling, thereby artificially reducing the particle number concentration in the standard. Additionally, particles may adhere to the stock containers during storage, which could also result in particle losses. Particle loss in the standard would underestimate the particle number introduced into the ICP-MS and thus lead to underestimation of the transport efficiency. Errors in particle number are directly related to the particle mass computed by Equation 1. Thus, if 50 % of the particles in the standard are lost due to sorption, an extreme example, the computed particle mass will be larger by a factor of 2. The reported diameter will be increased by 25 % (the cube root of 2). Finally, this approach for size analysis requires that losses during transport from the sample container to the plasma are identical for both the NP standard and any dissolved standards that may be used for calibration.

Method 3 is the particle size method, which utilizes the ratio of solution sensitivity and NP sensitivity to determine the transport efficiency. The signal from a solution is directly dependent on the transport efficiency, while the signal from an individual NP is not (only the number of detected NP events depends on the transport efficiency). Therefore, the ratio of the solution sensitivity (counts per ng of analyte delivered to the nebulizer) to the NP sensitivity (counts per ng of analyte in a single nanoparticle) is equal to the transport efficiency. This can be represented by Equation 3, which shows that the transport efficiency

is the quotient of the signal-to-mass ratios of both the dissolved standard solution and the nanoparticle standard,

$$\eta_{neb} = \frac{\frac{I_{STD}}{M_{STD}}}{\frac{I_{NP}}{M_{NP}}} \quad (3)$$

where

η_{neb}	nebulization (transport) efficiency
I_{STD}	signal from standard solution
M_{STD}	mass of standard solution delivered to the nebulizer
I_{NP}	signal from nanoparticle
M_{NP}	mass of nanoparticle

This method requires the size, density, and shape of the standard nanoparticle to be known. Nanoparticle standards are generally spherical and a measured diameter is always reported by the manufacturer, although the uncertainty in this information may vary among suppliers. To use this approach, the density is usually assumed to be equal to the materials bulk density. There are reports that this is not always true, with measured values being less than the bulk value [45]. A 2-fold error in density, perhaps larger than expected for bulk versus nanoparticle, has the same effect on diameter calculation as a 50 % loss of NPs in the standard solution when using method 2 (i.e., a 25 % overestimate of diameter). Finally, the other assumption is that the generation and transport of ions from the particle and the dissolved ions in a droplet is identical and that the sensitivities (counts/fg) are the same for both. If this latter condition is not met, then η_{neb} determined by method 3 is really a term that combines the actual transport efficiency (directly obtained from method 2) with a correction factor (CF). Thus one could consider:

$$\eta'_{neb} = \eta_{neb} \times CF \quad (4)$$

With respect to size analysis, using a transport efficiency obtained by this method should be more accurate if all NPs, regardless of composition, have similar CFs. Further work is needed to determine if the CF varies among NPs containing elements with differing volatilization and ionization behavior. If the value of CF is sufficiently large, use of η'_{neb} to determine particle number concentrations, instead of that obtained by method 2, could lead to errors. The magnitude of this error is directly related to how different CF is from a value of one.

Sample analysis considerations

Particle coincidence and dissolved analyte interference

A significant advantage in using spICP-MS is the ability to analyze particles in complex matrices without significant sample preparation. Where conventional ICP-MS analysis

requires samples to be acidified and possibly filtered prior to analysis, spICP-MS forgoes these preparation steps when possible, so long as the samples are capable of being aerosolized by the pneumatic nebulizer. While other analytical techniques may introduce analysis artifacts such as aggregation, dissolution, and other changes to nanoparticle stability and structure, spICP-MS analyses are able to characterize and quantify the nanoparticle analyte in its native media, although dilution is often utilized. This allows for a direct examination of transformation processes such as the aggregation state of the nanomaterial, and other physicochemical properties such as size, shape, and elemental distribution of the particles. However, there are some key aspects to consider in spICP-MS in order to achieve accurate and meaningful results.

The number of NP/mL in a sample can be determined by dividing the measured number of detected particle events per second by the transport efficiency and then dividing that result by the sample flow rate to the nebulizer (mL/s). However, the transport efficiencies measured by methods 2 and 3 are often not the same. The value obtained by method 2 contains no assumptions about the generation of ions from the NP and the dissolved standards being identical. However, having confidence in the “true” particle number can be difficult. In instances where the particle number concentration is too high relative to the selected dwell time, ‘coincidence’ can occur, where more than one particle is detected within a single dwell. This results in the apparent detection of fewer and larger particles, which both misrepresents the size distribution of the particle and underestimates the particle number concentration. In the early stages of single particle method development, when 3–20 ms dwell times were used, coincidence was prevented by working at low particle number concentration (i.e., 5 % of total readings are NPs) [39, 46–48].

As dwell times have become shorter, higher particle number concentrations can be analyzed as multiple particle events can be resolved. This is particularly evident at microsecond dwell times, where the breadth of each individual particle event can be quantified [49–51]. Though moving to shorter dwell times generally results in apparent ‘split events’, where a particle event is distributed among consecutive dwells [52], current data processing schemes account for this distribution of particle intensity and are capable of fully integrating the particle signal.

Even for sub-millisecond dwell times, in order to minimize the possibility of signals from two nanoparticles occurring within a single dwell time, it may be necessary to dilute the sample. The probabilities of the measured signal having contributions from zero nanoparticles, one nanoparticle, two nanoparticles, etc., depends on the number of nanoparticles per mL, the transport efficiency into the ICP, the dwell time, and the NP signal duration. The probabilities can be easily calculated from: $P_x = \frac{\lambda^x}{x!} e^{-\lambda}$, where x is the number of nanoparticles that will contribute to the measured signal and λ is the number of nanoparticles entering the plasma per second

times the larger of the dwell time or the signal width in time. It is generally observed that the duration of a pulse generated by each NP, regardless of its size, is on the order of 200–500 μ s. Thus, a practical upper limit is to have no more than one NP detected per 1–5 ms.

In addition to particle coincidence, the presence of dissolved analyte at sufficiently high concentrations can also affect the accuracy of spICP-MS measurements. Though spICP-MS is capable of distinguishing the pseudo-constant signal of dissolved analyte from the intermittent pulses of nanoparticle events, too high of a background signal from dissolved analyte or spectral overlap can mask particle events. The use of 100 μ s or shorter dwell times has improved this situation over that seen for millisecond dwell times, as the background signal is divided up proportionally into a greater number of dwell times. When the dwell time is reduced to less than the NP-generated pulse duration, which is contained in 2–6 dwell times, the only background contribution comes from that beneath the pulse, and not from dwell times between the pulses, as was the case for millisecond dwell times. This approach is also effective at reducing the effects of isotopic overlap with the analyte. Alternatively, the signal from dissolved analyte can be reduced or possibly eliminated by coupling ion exchange chromatography to spICP-MS in order to remove the dissolved analyte [53].

Matrix effects and matrix matching for calibration

One of the most pressing issues with regard to spICP-MS is the effect of the sample matrix on the analysis of NPs. Moreover, how the matrix affects the conversion of NPs to signal relative to the conversion of dissolved analyte to signal has significant implications for spICP-MS accuracy. This is immediately relevant to the determination of the transport efficiency, where sample matrix (high concentrations of dissolved solids, acid(s), or organic solvents) can differently impact the sensitivity from elements that are dissolved and elements present in nanoparticles. Montoro Bustos et al. [54] reported large, matrix-dependent changes in Au sensitivities from solutions and from nanoparticles that were often different from Au present in a NP compared with Au in solution (Table 1). In an extreme case, solutions that contained 0.05 % Dulbecco’s Eagle medium (DEM) suffered a 90 % decrease in the Au solution sensitivity but had little effect on the nanoparticle sensitivity. This is consistent with instability of dissolved Au in DEM, resulting in loss of dissolved Au.

If calibration solutions are not matched to the sample matrix, this may result in an error in the measured nanoparticle diameter corresponding to the cubed root of the relative sensitivity, as mass is related to particle volume (Equation 3). Montoro Bustos et al. [54] demonstrated that when calibration solutions and nanoparticle suspensions were matrix matched, they were able to obtain accurate nanoparticle diameters using

Table 1 Effect of different sample matrices on Au solution and nanoparticle sensitivities [54]

Matrix	Change in solution sensitivity due to matrix (relative to DI H ₂ O matrix)	Change in nanoparticle sensitivity due to matrix (relative to DI H ₂ O matrix)
10 mM Phosphate buffered saline	−70 %	−75 %
1 % Methanol	+45 %	+30 %
10 mM Sodium lauryl sulfate	−5 %	−30 %
100 mg/L Natural organic matter	−15 %	<±1 %
0.05 % Dulbecco's Eagle medium	−90 %	<±1 %

method 3 (“particle size” method) to determine the transport efficiency. However, the transport efficiencies measured using method 3 were often very different than those using method 2 (particle number method) in the matrix matched calibration solutions and nanoparticle suspensions. This discrepancy between transport efficiencies determined by methods 2 and 3 was a systematic problem through analyses and led to erroneous results in sizing and counting when the transport efficiency was in error.

In addition to the complications arising from complex biological and environmental matrices, some analyte elements may not be stable in deionized water so that solutions used for calibration using method 3 (“particle size”) may need to contain acid when the nanoparticle suspensions do not. The sensitivities (counts/ng of analyte element entering the plasma) in solutions or suspensions with acid will likely not be the same as in solutions or suspensions without acid.

Olesik et al. [2016 WC] found that Au solution sensitivities increased by a factor of 200 % as the HCl concentration was increased from 0 to 2 % v/v while the nanoparticle sensitivities changed by less than 3 %. (Si coated Ag NP were used and did not dissolve in 2 % v/v HCl). If the transport efficiency determined by method 3 was used in combination with the sensitivity determined from solutions, the correct nanoparticle diameter was obtained, even if the solutions contained 2 % v/v HCl and the NP suspensions did not. However, if method 2 was used to determine the transport efficiency and Au solutions were used to measure the sensitivity, the nanoparticle size results were about 20 % too low. Furthermore, when matrix matched solutions and suspensions that both contained 2 % v/v HCl, erroneous results were still obtained using method 3 to determine the transport efficiency together with Au calibration solutions to determine sensitivity.

In conjunction with errors in sizing, measured nanoparticle number concentrations were correct only if the transport efficiency measured using the particle number method (method 2) was used. When the particle size method (method 3) was used to determine transport efficiency, the NP number concentrations were too low by almost a factor of 2. When an internal standard, added to both the solutions and nanoparticle suspensions was used, matrix induced changes in the measured

nanoparticle size were reduced to less than 4 % and matrix induced changes in the particle number concentration were reduced to less than 10 % even when the solutions contained 2 % v/v HCl and the nanoparticle suspensions did not. An internal standard has also been used to account for drift in instrument sensitivity during spICP-MS [55, 56]. Clearly further work in assessing the effects of matrix-matching of dissolved and NP-containing solutions is needed to assess their effect on the accuracy of sizing and counting NPs.

Data acquisition and processing

Peak identification and integration

Prior to calculation of the particle size distribution and number concentration from the NP pulse intensity and frequency, respectively, the NP events (i.e., signal peaks) must be separated from the background signal (i.e., instrument noise and signal from dissolved analyte elements). Two data processing methods exist to distinguish NP events from the background: (1) a well-established iterative approach using a background threshold value above which signal intensities are identified as NP events, as presented by Pace et al. [39], and (2) a more recent signal deconvolution method developed by Cornelis and Hassellöv [57].

ICP-MS manufacturer nano-application software modules are at this point typically based on the iterative approach. As described by Pace et al. [39], when 3–20 ms dwell times are used and a NP event is represented by only one intensity (contained in one dwell time), data points above the mean plus 3σ of the entire data set are identified as NP pulses and removed. The averaging process and peak removal process is iterated until there are no more data points above the threshold. The mean of the data set plus 3σ is typically chosen as the threshold because it is the same method commonly used to remove outliers from a normally distributed data set (it is assumed that the background data points have a normal or near-normal distribution), although other threshold values, such as the mean plus 5σ , have been used [46, 51]. Following the iterative

removal of all NP events from the raw data set, the remaining data represent the background signal from which a dissolved metal concentration can be determined. The sum of the number of NP pulses above the threshold is the total number of detected particle events.

When using microsecond dwell times, most commonly less than or equal to 100 μs , for which a NP event is composed of multiple consecutive readings above the background, a similar process is used. However, an additional requirement is that following NP event identification, the consecutive signal intensities that constitute a single NP event must be summed to obtain a total NP intensity. The iterative method works well for large NPs for which the signal intensities are clearly above the threshold; however, for small NPs and/or samples with a high ionic background, useful particle detection and characterization are more difficult, and in some cases impossible. Alternative methods may be used to better discriminate (small) NPs from a (high) dissolved background signal. Cornelis and Hassellöv [57] developed a signal deconvolution method using Polygaussian probability mass functions to separate the contribution of ion signals attributable to NPs from the signal intensity due to particle ions and dissolved ions within the given dwell time.

When signals from NPs measured with dwell times $\leq 100 \mu\text{s}$ are very small (with little or no background), shot noise can result in the signal from a single nanoparticle going above, below, back above, and then below the threshold. This can result in an overestimate of the total number of NP events and an underestimate of the size of NPs require more sophisticated data processing tools in order to distinguish NP signal from noise.

Conversion of spICP-MS signal to NP size

The signal intensities collected from the ICP-MS are converted to mass using the aforementioned mass flux calibration curve (Equation 1). The slope of the curve is used to convert the signal intensity to a mass as shown in Equation 4. If the particle analyzed consists of more than one element, the mass fraction is used to convert the signal from the singular element to an overall mass of particle [30, 39],

$$M_p = \frac{1}{f_a} * \frac{[I_{NP} - I_{BKGD}]}{m} \quad (5)$$

where

M_p	mass of the particle
f_a	mass fraction (fraction of particle mass due to the analyte element)
I_{NP}	Signal intensity from nanoparticle event
I_{BKGD}	Signal intensity of the background
m	slope of the mass flux curve

The mass can then be converted to a diameter for NPs if the density of the material is known (Equation 4) [39],

$$D_{NP} = \sqrt[3]{\frac{M_p * 6}{\rho * \pi}} \quad (6)$$

where

D_{NP}	diameter of the particle
M_p	mass of the particle
ρ	particle density

This conversion from nanoparticle mass to size conversion is not limited to spherical particles, however, as the length of silver nanowires has been calculated if the diameter of the cylinder is known [58], using the appropriate equation to relate the nanoparticle mass to volume.

In many cases, the particle density has been assumed to be the bulk density of the material being analyzed. Recent studies have shown that the density of some particle compositions may be size-dependent [59, 60]. Falabella et al. demonstrate through analytical ultracentrifugation that as the size of gold NPs decrease, the density also decreases [45]. The potential for size-dependent particle density is an emerging aspect of spICP-MS that needs further consideration as it continues to develop into a routine analysis technique.

Influence of instrument components on spICP-MS signal and data quality

In order to discuss spICP-MS as a powerful analytical technique, as well as consider its limitations, it is worthwhile to examine the operational aspects of ICP-MS [61–65]. Many of the components of an ICP-MS analysis will affect nanomaterial measurements including the transport of nanoparticles into the plasma, the intensity and duration of ICP-MS signals, and the percentage of ions transmitted from the plasma to the detector [66].

Sample introduction

Samples to be analyzed by ICP-MS are typically introduced as an aerosol into the plasma via a nebulizer. Pneumatic nebulizers, operated at sonic gas velocities, are typically used to generate the sample aerosol, with a range of droplet sizes from $<1 \mu\text{m}$ to more than $20 \mu\text{m}$ in diameter [67]. If all of the sample were to enter the plasma, the solution load would be too high to maintain the plasma temperature in the central channel through which it travels. Furthermore, under commonly used plasma conditions, $20 \mu\text{m}$ droplets are not completely vaporized in the ICP [34]. Therefore, a spray chamber is used to limit the amount and reduce the size of

the droplets that enter the plasma, both of which have impacts on the analysis of NP size and number.

The key processes in the spray chamber that determine whether or not a droplet enters the plasma are droplet evaporation, droplet impact on the walls, and droplet–droplet coagulation. The more extensive the droplet evaporation, the smaller the droplet becomes and the more likely it is to be retained in the fraction of gas entering the plasma. Larger droplets are more likely to impact on the walls of the spray chamber and thereby be removed. Droplet–droplet collisions can result in their coalescence into a larger droplet, which favors impact on the walls. While the largest droplets are removed in the spray chamber, the aerosol exiting the spray chamber remains polydisperse.

The analyte transport efficiency, discussed previously with respect to calibration, decreases as the sample uptake rate is increased. Typical transport efficiencies decrease from around 15 % at a sample uptake rate of 0.1 mL/min to around 1.5 % at 1 mL/min [68, 69]. At sample uptake rates ≤ 10 $\mu\text{L}/\text{min}$, transport efficiency can be as high as 100 %, with typical transport efficiencies in open, conical spray chambers or double pass spray chambers of 60 to 80 % [68–70]. Transport efficiencies near 100 % are possible for flow rates up to 0.5 mL/min when using some spray chamber designs, including heated spray chambers with solvent vapor removal [71] and unheated spray chambers used with low (~ 10 $\mu\text{L}/\text{min}$) sample uptake rates [72]. At sample uptake rates ≤ 10 $\mu\text{L}/\text{min}$, evaporation of the droplets in the spray chamber is more extensive (up to 25 mg L^{-1} of water vapor per L of Ar at room temperature) and the probability of droplet–droplet collisions/coagulation decreases rapidly as the number of droplets generated per second decreases. Baffled cyclonic spray chambers typically have lower transport efficiencies (~ 30 %) at sample uptake rates ≤ 10 $\mu\text{L}/\text{min}$ because the spray is directed at the wall of the spray chamber, in contrast to open conical or double pass spray chambers. Furthermore, if the sample matrix affects the surface tension of the solution, in turn affecting the droplet size distribution or the rate of droplet evaporation in the spray chamber (methanol addition for example), the transport efficiency could be different than for pure, deionized water.

Micro-droplet generators have also been used to generate aerosols from nanoparticle suspensions with nearly 100 % efficiency. This provides for an approach to measure spICP-MS sensitivity (counts/fg analyte element) without the need for nanoparticle standards of known size [36, 73, 74]. Monodisperse droplet generators typically produce droplets (30 to 60 μm in diameter, depending on the generator design and voltages applied) that are too large to be completely vaporized in the ICP under typical plasma conditions. Therefore, a desolvation system is often used prior to introduction of the droplets into the ICP. One example uses He in a long tube to allow droplets to evaporate at a much higher rate than in Ar without the need for heating [36, 75]. Monodisperse droplet

generator designs include a capillary surrounded by a piezoelectric tube that ejects a droplet when a voltage pulse is applied, a microfluidics based droplet dispenser [76], and thermal ink jet printer-like designs [77].

Conversion of droplets and nanoparticles into elemental ions in the plasma

The properties of the plasma dictate how much sample can be introduced into the plasma without excessively cooling or extinguishing it [78]. Heat transfer from the outer “energy addition” region of the plasma to the sample-carrying center channel, the kinetics of droplet evaporation, and the kinetics of nanoparticle vaporization determine what size aerosol droplets and what size NPs will be fully vaporized and converted to elemental ions.

Each aerosol droplet undergoes a sequence of processes during the ~ 1 to 3 ms it travels through the ICP, including droplet desolvation, vaporization of the remaining particle (nanoparticle and any other dissolved solids in the sample), atomization, ionization, and diffusion of ions in the plasma prior to being sampled by the mass spectrometer [66], as shown in Fig. 2.

The polydispersity of droplets entering the plasma affects desolvation and production of signals from NPs. Large droplets will complete desolvation farther downstream in the plasma than small droplets. Therefore, nanoparticle vaporization will begin farther downstream and the resulting ion cloud will have less time to diffuse before reaching the sampling orifice compared with ions produced from a nanoparticle that was carried into the plasma in a smaller droplet. This could introduce some variation in the intensity and duration of ICP-MS signals from NPs of the same size and therefore result in NP size distributions that are broadened. Fluctuations in the plasma gas velocity could also introduce similar variations.

The local plasma surrounding each vaporizing droplet and particle is cooled by the desolvating droplet and vaporizing particle [79, 80]. Sufficient time is required in the hot ICP to completely vaporize the nanoparticles [31, 81, 82]. After vaporization, atomization, and ionization, a cloud of mainly elemental ions (for the majority of elements in the Periodic Table) is produced [83, 84]. The location along the center channel where vaporization and ionization are complete can depend on the chemical composition and size of the particles, particularly for particles that are much greater than 100 nm in diameter [32].

Ion diffusion in the plasma: impact on ion cloud diameter and ICP-MS signal duration

When operating conditions of the sample introduction system are optimized for maximum ICP-MS signal creating

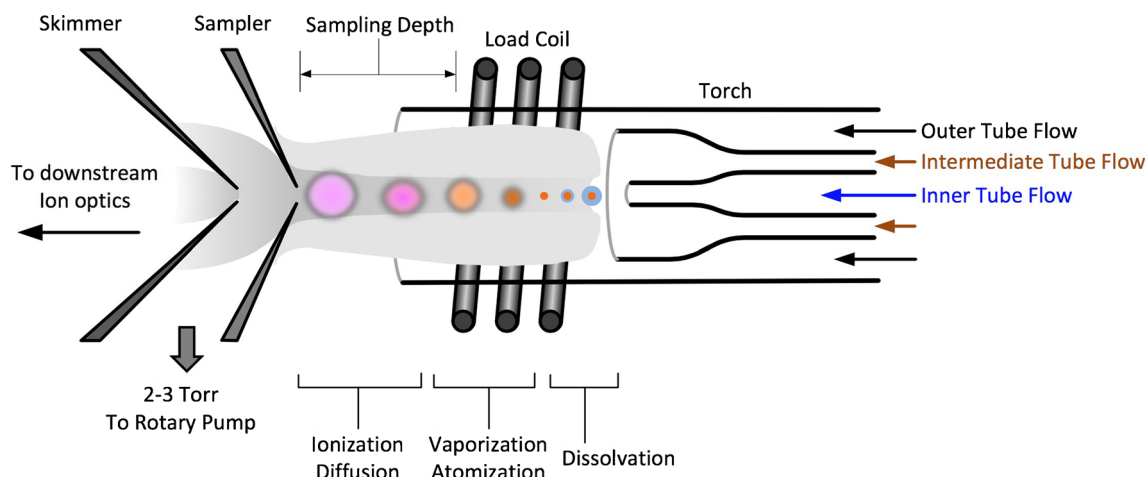


Fig. 2 Droplet desolvation, atomization, and ionization in the plasma. Figure courtesy of H. Badiei, Perkin Elmer Inc.

monodisperse droplet injection into the radial center of the center channel of the plasma, the ion cloud is approximately 4 to 10 mm wide when it reaches the sampling orifice [84, 85]. At a typical plasma gas velocity of ~ 20 m/s, the duration of the particle-generated signal peak is therefore typically 200 to 500 μ s. More typically, signals from nanoparticles introduced using a pneumatic nebulizer have been reported to be from 100 to 1000 μ s in duration [42]. The duration of the NP event is important in that longer times spread the generated counts out among more dwell times, resulting in a lower signal above background. Signal duration is also important for the development of dual element detection capabilities using a fast peak hopping quadrupole mass spectrometer as described in a subsequent section.

The width (in time) of the ICP-MS signal produced from each nanoparticle arises mainly from the extent of diffusion of the ion cloud, which depends on isotope mass and the time that the ions spend in the plasma prior to passing through to the sampling orifice [31, 84, 85]. At a particular location along the center axis of the plasma there is a sharp transition from cold (<500 K) to hot (~ 6000 to 8000 K) plasma gas [31, 71, 86]. The time that the sample spends in the hot plasma depends on the location of the transition point, the distance from that point to the sampling orifice (sampling depth), and the plasma gas velocity. The rapid sequence of processes, starting with droplet desolvation, begins when the droplets enter the hot plasma. While the nanoparticle is vaporizing, the nanoparticle is a local source of ions and the full width at half maximum of the ICP-MS signal will be narrow [31]. Once the nanoparticle has been completely vaporized and converted to elemental ions, the full width at half maximum of the ion cloud will increase with time spent in the plasma [31].

At a fixed plasma power and a particular torch injector inner diameter, the key experimental parameter that determines the location of the transition from cold to hot plasma in the center channel of the plasma is the center gas flow rate (nebulizer gas plus any additional “make-up” gas that passes

through the torch injector tube) [71, 86]. When the center gas flow rate is increased, the location where the transition from “cold” to “hot” occurs along the center channel (axis) moves downstream (closer to the sampling orifice), resulting in a shorter time that the sample spends in the hot plasma. As a result, if a nanoparticle is completely vaporized, the width (duration) of the ICP-MS signal will increase, due to more time for diffusion, as the center gas flow rate decreases [31, 85]. Perhaps somewhat non-intuitively, increasing the center gas flow rate has only a small effect on the hot plasma gas velocity and temperature downstream of the transition location. The ratio of a molecular oxide ion signal to the elemental ion signal (e.g., CeO^+/Ce^+ or UO^+/U^+) typically does not change dramatically as the center gas flow rate is increased until the location of the transition from “cold” to “hot” gets too close to the sampling orifice. Therefore, the main effect of changing the center gas flow rate is to shift the location of the transition from cold gas to hot plasma upstream or downstream relative to the sampling orifice. In some cases, the travel time through the hot plasma can also depend on the path that sample takes through the plasma, which may not be along a straight line [87, 88]. For elements of different volatility, this can affect the arrival time of their ion clouds at the sampling orifice [89].

Background reduction using collision/reaction cells

Collision/reaction cells are widely used for solution ICP-MS to overcome spectral overlaps. However, collision/reaction cells have only recently been used for spICP-MS measurement of nanoparticles [52, 90–92]. The need for removal of spectral overlap by collision/reactions cells is somewhat lessened by the use of short signal integration times, which increases the ratio of NP analyte signal to the spectral overlap signal. Unless the spectral overlap ion is originating from elements in the NP, the spectral overlap background signal will

decrease as the dwell time approaches or becomes less than the NP signal peak duration. Measurement of elements (such as iron) that suffer from intense spectral overlap ion signals (such as $^{40}\text{Ar}^{16}\text{O}^+$ at the same nominal mass of $^{56}\text{Fe}^+$) could still benefit from the use of a collision/reaction cell [93].

Ion transmission to the mass spectrometer: effect on ICP-MS sensitivity

While most or all of the ion cloud passes through the sampling orifice [94], only a small fraction of the ions and plasma gas pass through the skimmer orifice into the lower pressure region ($\sim 10^{-4}$ Torr). The transport of ions through the interface is thought to be dictated mainly by the flow of neutral Ar atoms [95, 96] although recent research suggests that this may not be entirely true. The ICP-MS signal intensity arising from a given mass of analyte and, thus, the size detection limit of single particle ICP-MS, will depend on the ion transmission efficiency from the sampling orifice to the mass analyzer.

Downstream of the skimmer orifice, a positive ion beam is formed. The positive ions in the beam repel each other. The number of ions in the beam is large enough so that many of the ions in the positive ion beam are lost because of space-charge repulsion or shielding [97]. Space-charge effects explain the mass-dependent ion transmission efficiencies to the mass analyzer. The ion transmission efficiencies can be greatly reduced by high concentrations of concomitant elements in the sample (i.e., mass dependent matrix effects) [98], likely due to space-charge effects. Therefore, the sample matrix may affect the relationship between nanoparticle signal peak area and the nanoparticle size.

Signal measurement

The spICP-MS technique relies on NPs creating short-duration pulses with intensities greater than the background signal. Identification and measurement of signals arising from individual NPs, especially in the presence of dissolved analyte element or polyatomic interferences, is best done by making multiple measurements during the duration of the 100 to 1000 μs wide signal generated by individual NPs [42].

Continuous measurement with $\leq 100 \mu\text{s}$ dwell times

Continuous, rapid measurement of signals with dwell times of 100 μs or less is ideal. Most current commercial ICP-MS instruments using quadrupole mass spectrometers provide this capability, although it is also possible to make measurements using instruments with slower detection systems common on previous generations of ICP-MS instruments.

Non-continuous measurement with 3–20 ms dwell times

Traditionally (in previous generations of ICP-MS instruments), detection electronics on commercial ICP-MS instruments were not designed to make continuous measurements on the tens of microseconds time scale because signals from solutions were typically integrated for 10 to 1000 ms. Minimum dwell times of 1 or 10 ms were common. Furthermore, many commercial instruments required time to process each measurement during which signal was not measured (or had a built-in delay after each measurement intended to allow settling of the fields in the quadrupole mass analyzer after peak hopping from one mass to another), so the measurements were not continuous.

In that case, a long enough dwell time is needed to minimize the possibility of detecting only a portion of the 0.2 to 0.5 ms wide signal from an individual nanoparticle (more likely for a dwell time of 1 ms than for a dwell time of 20 ms) while maximizing the ratio of signal of an individual nanoparticle to the signal from the element in solution (better for shorter dwell times).

The signal from elements in solution is quasi-steady state (although with significant variation on the ms or sub-ms time scale). Therefore, the average number of counts from an element in solution will increase linearly with dwell time while the signal (counts) from an individual nanoparticle will not change as the dwell time is decreased from 1000 ms to 1 ms (assuming there is only signal from only one nanoparticle during the dwell time).

External electronics for continuous, rapid (microsecond) pulse counting signal detection

In order to provide high speed ($\leq 100 \mu\text{s}$ per measurement) pulse counting measurements using older generation ICP-MS instruments, external electronics have been used by some researchers. Strenge and Engelhard [99] used a home-built data acquisition system with dwell times as small as 5 μs and a large buffer memory to acquire data continuously over long times. Details on the specific electronic components used were not provided. Miyashita et al [100] used commercially available National Instruments components to process and store the pulse counting signals with dwell times as short as 1 μs .

Limited dynamic range of pulse counting detection of individual nanoparticles

The dynamic range of pulse counting detection is limited on the high end by the ~ 10 –50 ns detector dead time because of the width of the pulse of electrons produced from each ion that

strikes the secondary electron multiplier detector and any subsequent electronics (amplifiers, comparators, etc.) prior to the counting electronics. This results in a nonlinear response for intense signals from individual nanoparticles [81]. For a detector and processing electronics with a dead time of 50 ns, a peak signal of 2,000,000 c/s, corresponding to just 100 counts in 50 μ s, would on average result in a measured signal of 90 counts (i.e., a 10 % error). As Strenge and Engelhard point out [99], the error attributable to this detector “pulse pileup” would be worst at the peak of the signal from an individual nanoparticle when the signal is largest and less severe for the signals before and after the peak of the signal. If the signals from individual nanoparticles are too large to be within the dynamic range of the pulse counting system, the sensitivity (counts/fg) could be reduced by increasing the resolution provided by the quadrupole mass analyzer, detuning the ion beam focusing optics, or using a collision gas at a high enough pressure (flow rate) to cause ion scattering losses [52].

When dwell times of 100 μ s or less are used and the sample contains a low concentration of dissolved analyte, the blank signal can be zero counts. In that case the smallest, reliably detectable signal is not limited by the fluctuations in the blank signal but rather by the instrument sensitivity and shot noise.

Analog measurement of nanoparticle signals

If the signal is too large to be measured by pulse counting, electronics analog measurement could be used. However, the analog detection electronics on most of the commercial ICP-MS instruments cannot accurately measure and convert analog signals to digital values within 100 μ s or lesser measurement times. The current to voltage amplifier in the ICP-MS may respond fast enough but the digitizer may not be capable of short enough conversion times. If the current to voltage amplifier in the ICP-MS is fast enough, an external digital oscilloscope or fast analog to digital computer board can be used to digitize the signal from the current to voltage amplifier in the ICP-MS. Alternatively, the analog output of the detector could be directly connected to a digital oscilloscope [36, 101] or to a fast external current to voltage amplifier followed by a digital oscilloscope [31, 79, 85]. The digital oscilloscope can be connected to a computer for data processing. Analog detection will not be able to measure signals from as small NPs as pulse counting detection systems but can easily provide time resolution to 1 μ s in order to investigate the shape of the signal versus time in detail.

Recent Advances in Instrumentation and Data Processing

In the past decade, spICP-MS has developed from a niche technique to a powerful tool for the analysis of nanomaterials

[30]. Though it still suffers from a number of limitations, a great deal of research has been performed in the last 5 years in order to overcome some of these initial hindrances. Continued research on both the hardware and software aspects of ICP-MS, and specifically spICP-MS, will further improve the applicability of this technique toward a wider array of research problems.

Progress toward automated data processing

One of the largest contributors to the growing use of spICP-MS in recent years has been the development of automated data processing software provided by many of the major ICP-MS suppliers [102–105]. These software packages automate many of the processes in single particle analysis, from determining the transport efficiency, calculating the diameter of the analyzed particles, and creating histograms to show the size distribution. As many of the inputs are user-defined (e.g., dwell time, mass fraction, particle density), a wide breadth of nanomaterials can be analyzed without the need to manually perform the data analysis. In addition to particle sizing, these application modules also automatically calculate metrics such as particle number concentration and dissolved analyte concentration, further adding to the wealth of information gleaned from spICP-MS analysis.

Hyphenation: a route toward data enrichment

In environmental and biological samples, the presence of naturally-occurring colloids and complex matrices can complicate the detection and characterization of engineered NPs [28]. A front-end size fractionation technique such as field-flow fractionation or hydrodynamic chromatography may be useful in allowing for spICP-MS analysis on a size basis. Loeschner et al. investigated the applicability of using asymmetrical flow-field flow fractionation (AF4) to overcome challenges in analyzing silver NPs in enzymatically digested chicken meat [106]. By comparing both the total size distribution of NPs before and after size fractionation, they were able to demonstrate approximately 80 % recovery. This technique has also been used to characterize metal wear particles in serum samples that were released from hip aspirates. In doing so, the size distribution and particle number concentration of chromium, cobalt, and molybdenum containing particles were determined [107]. In addition to flow-FFF, sedimentation-FFF has also been used to separate polydisperse nanoparticle distribution, specifically titanium dioxide NPs [108]. This technique may be particularly useful in instances where particles may share the same size and composition but possess different masses (i.e., core-shell particles, porous versus non-porous particles).

Hydrodynamic chromatography (HDC) has also been applied to separate particles prior to analysis by spICP-MS.

Though this technique does not have the level of resolution that FFF possess, it is not subject to the same analysis artifacts (membrane interactions) that can lead to low recoveries. Using HDC, Roman et al. investigated the presence of silver NPs in human serum samples obtained after treatment with nano-enabled medical dressing [109]. This method was also applied to environmental samples, where the presence of naturally occurring particles may either directly (same composition) or indirectly (aggregation, dissolved analyte) interfere with the detection of NPs [110].

Other environmental complications such as dissolved analyte may also obscure the detection of engineered NPs. To overcome this, Hadioui et al. coupled ion exchange chromatography (IEC) prior to analysis by spICP-MS in order to remove signal from dissolved analyte [53, 111]. For NPs that have shown a propensity to dissolve readily in environmental samples such as silver [112] and zinc oxide [113], IEC is used to greatly improve the resolution of nanoparticle signals from an elevated background signal emanating from dissolved analyte, thereby improving size detection limits. With these further advances in the development of front-end fractionation techniques, the applicability of spICP-MS to environmental and biological samples can be greatly improved.

Particle-by-particle multi-element detection

Many applications of spICP-MS highlight the power of this technique to characterize engineered nanomaterials in a variety of complex matrices, though most spICP-MS work to date has focused on detecting particles by focusing on a single mass. However, in environmental samples, the concentration of naturally occurring nanomaterials is much greater than the expected environmental release concentrations of ENPs. Furthermore, many of these natural particles are comprised of these same elements the ENPs contain. In order to differentiate these two particle populations, it will be necessary to examine other delineating properties that differentiate engineered and naturally occurring nanomaterials [28].

A promising method is to examine the elemental ratios on a particle-by-particle basis, as engineered particles are typically enriched in a set proportion of elements, contrasting with the heterogeneous composition of naturally occurring nanominerals. To quantify these elemental ratios, two different modifications can be applied to spICP-MS methodology in order to observe multiple elements within a nanoparticle event.

One way is to shorten the settling time on the quadrupole of the ICP-MS to allow two elements to be monitored within a nanoparticle event ($\sim 500 \mu\text{s}$). At short dwell times and settling times ($100 \mu\text{s}$ or shorter), this allows at least two points of intensity to be detected on a particle-by-particle basis. This is shown in Fig. 3a, where dwell time A depicts the passage of ions for the first monitored mass. The settling time required to

switch from one mass to another results in losses of both ions. Dwell time B then allows for the passage of the second monitored mass. This results in nanoparticle events that exhibit some intensity of both masses as shown in Fig. 3c. On a qualitative basis, this may be used to differentiate between engineered particles that may contain only one element from their naturally occurring counterparts that contain multiple elements. Quantitatively, the total sum of intensities can be used to calculate the isotopic/elemental ratio of the samples as has been shown with silver NPs, core-shell NPs, and river samples containing ceria NPs [28, 50].

Another emerging technique is ICP-time of flight-MS (ICP-TOF-MS) (Fig. 3B) [37, 74]. By using a time-of-flight mass analyzer, nearly all elements can be detected quasi-simultaneously on a particle-by-particle basis and with short detection dwell times ($\sim 33 \mu\text{s}$). As shown in Fig. 3d, this technique is able to differentiate between single metal and core-shell materials.

Single particle ICP-MS applications

As an analytical technique, spICP-MS has proven to be a powerful tool with a number of potential applications in industrial, biological, and environmental fields of study. As a high-throughput ensemble technique with the specificity of a single particle technique, spICP-MS has the ability to overcome many of the sampling artifacts and provide a wealth of information regarding particle size, size distribution, and concentration of dissolved analyte present in the sample. As this technique continues to develop, a greater number of questions regarding nanomaterial transformation and interaction with environmental particles can be answered.

Environmental detection and characterization

Diverging from its origins in atmospheric chemistry [11, 14], recent spICP-MS studies have mostly focused on its application to aqueous environmental samples [48, 114, 115]. The continued market growth of nanotechnology [116, 117] increases the potential for NP release into the environment through accidental industrial release [118, 119], purposeful application (e.g., nanopesticides) [120, 121], or release from consumer products into waste streams [115, 122, 123]. Studies investigating wastewater treatment plants (WWTPs) have used spICP-MS to detect a number of different nanoparticles (e.g., Ag, Ti, and Ce-containing NPs) in wastewater effluent, demonstrating some of the potential deficiencies in current treatment structures to completely eliminate nanoparticulate contaminants [48, 114]. A recent study investigating drinking water treatment facilities (DWTs) on the Missouri River show the presence of titanium dioxide NPs in the influent waters; however, this method demonstrated the removal

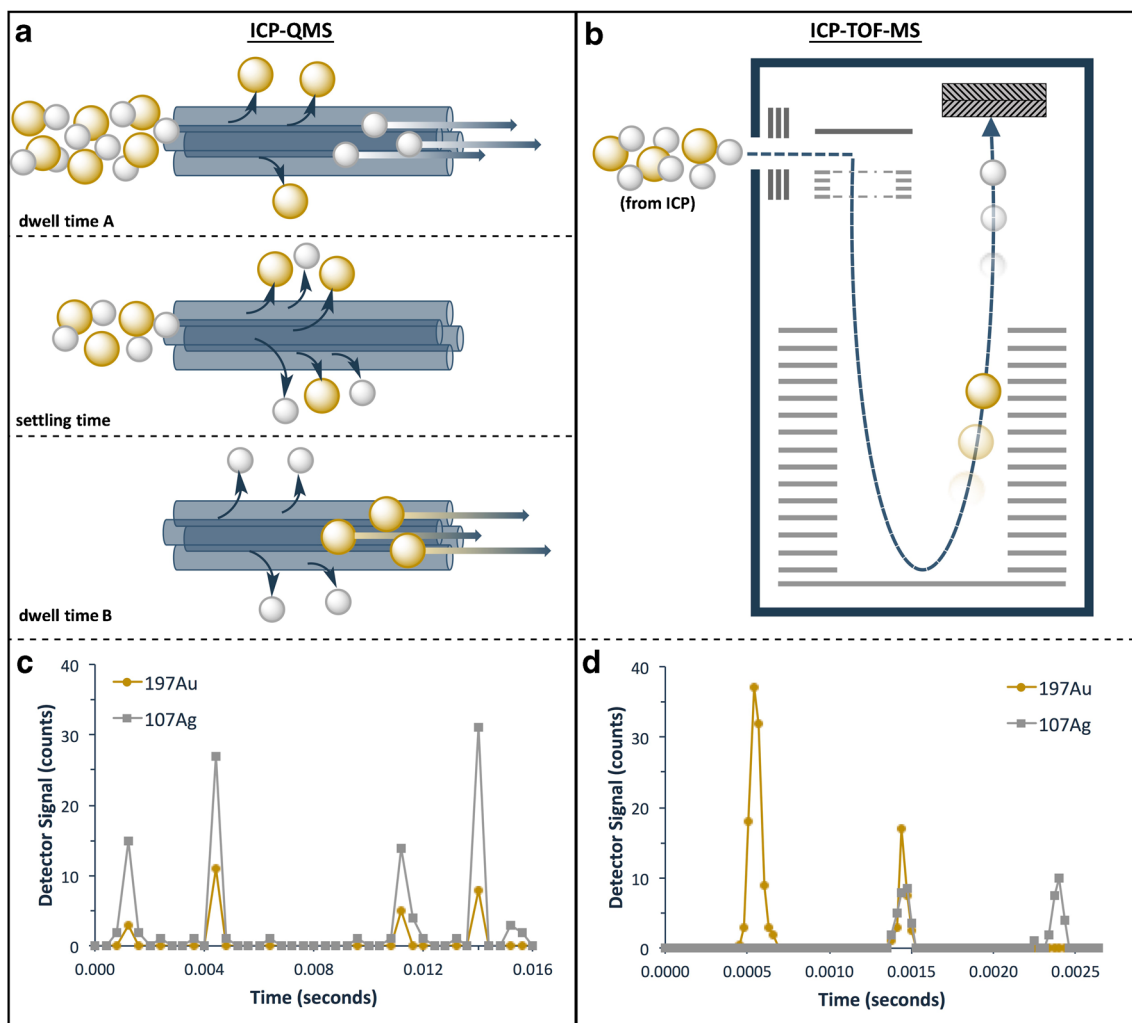


Fig. 3 Dual element spICP-Q-MS and ICP-TOF-MS. **(a)** Operation of fast-switching quadrupole allowing the passage of two different masses separated by a settling time. **(b)** Schematic of ICP-TOF-MS, where ions generated from a particle event are detected by a microchannel plate detector typically operated at 33 μ s dwell time. **(c)** Data from spICP-Q-

MS in dual element mode showing signal from two elements per particle [50], reproduced by permission of The Royal Society of Chemistry. **(d)** Data from ICP-TOF-MS showing signal distribution in gold, gold/silver, and silver nanoparticle events [adapted from Borovinskaya et al. [37] Copyright 2014 American Chemical Society

exceeding 93 % of NPs, resulting in levels safe for human consumption [124].

Recent studies have focused on the release of engineered nanoparticles (ENPs), specifically silver nanoparticles and titanium, from consumer products such as textiles, food packaging, sunscreens, and washing machine effluents [92, 115, 123, 125–131]. The prevalent use of titanium dioxide (TiO_2) in sunscreens ensures a high potential for release into the environment. The analysis of TiO_2 NPs in natural systems highlights some current deficiencies of spICP-MS in quantifying ENPs in the environment. In pristine environments, the size detection limit of TiO_2 NPs has been approximated at 100 nm. However, high ^{48}Ca content interferes with the detection of ^{48}Ti , resulting in a larger minimum size detection limit of approximately 130 nm. In addition, the high concentration of naturally occurring nanoparticles (NNPs) in

environmental systems requires a more sophisticated approach (elemental ratios) to distinguish ENPs from NNPs [28, 50, 115]. Though spICP-MS currently lacks the capability to distinguish between these particle populations, development of multi-element spICP-MS particle analysis (ICP-TOF-MS, dual element spICP-Q-MS) may result in methodology capable of detecting ENPs amidst NNPs.

One of the key strengths of spICP-MS is its ability to simultaneously detect particulate and dissolved signal at environmentally relevant concentrations [47, 50, 57]. The high reactivity of nanomaterials afforded by their increased surface area also makes them more susceptible to transformation processes such as dissolution and aggregation. Exploiting this capability to study particle transformation in their native environmental media is important as any additional sample preparation may alter the chemistry of the media, resulting in a

misrepresentation of particle behavior. Silver nanoparticle aggregation has been studied in simulated sea water, demonstrating the rapid aggregation these particles are subject to in high salinity solutions [132]. Dissolution of Ag NPs in different aqueous compositions has also been studied, quantifying the rate of dissolution of three types of Ag NPs with different surface coatings [112]. Using spICP-MS, the rate at which the diameter decreases can also be correlated to an increase in dissolved signal, allowing a mass balance to be calculated to ensure an accurate depiction of Ag NP transformation [112]. These dissolution processes have also been demonstrated in natural systems where Ag NPs were dosed into a littoral lake mesocosm [133]. This capability is also important for monitoring transformation of nanomaterials in consumer products. Figure 4 demonstrates the capability of spICP-MS to track the dissolution of silver nanoparticles in different types of detergent throughout the wash cycle [134]. The propensity for Ag NPs to both dissolve in the environment and be subject to alteration of their surface coatings, key transformation processes to consider when assessing the ecotoxicologic risk of these materials, were observed.

Biological uptake/medical applications

Another growing area of spICP-MS application is the study of nanomaterial exposure and transformation in biological systems. The use of NPs in food products, bioimaging, and medical treatments permits a feasible route for NP biological uptake and transformation. A frequent impediment in the analysis of nanomaterial in biological matrix is extracting the NPs into a phase where they can be analyzed. Conventional analyses would perform a complete digestion of tissue, thereby removing any capability to characterize the nano properties of the material (e.g., size, aggregation state, etc.). To study Ag and Au NP uptake into model aquatic organisms (*Lumbriculus variegatus*, *Daphnia magna*), Coleman et al.

[135] utilized sonication as a means to extract the metallic NPs from the organismal tissue. FFF-ICP-MS and spICP-MS were then used to characterize the size of the NPs suspended in the solution, showing a minimal size change but a considerable decrease in particle number concentration attributed to losses in particles attaching to the tissue.

Gray et al. [136] utilized tetramethyl ammonium hydroxide (TMAH) as a means to extract NPs without acidification. Silver and gold NPs were spiked into ground beef, *D. magna*, and *L. variegatus*, and extracted with TMAH, demonstrating high extraction efficiency (recoveries between 75 and 125 %). Using this method, it was demonstrated that different particle sizes could be resolved and that minimal size changes were observed over the time period investigated. Enzymatic digestion methods have also been used; proteinase K was used to extract silver NPs that had been spiked into chicken meat. The recovery of Ag NPs was high (80 %) and minimal size changes were observed during residence in the tissue [106, 126]. Enzymatic digestion has also been used to extract NPs from plant tissue. Tomato plants exposed to 40 and 100 nm gold NPs were digested and NPs extracted using macerozyme R-10 with good recovery, and results demonstrated no significant size transformation over the 4-d exposure period [137].

In some cases, NPs may be analyzed directly in their native media without the need for digestion. Figure 5 shows the distribution of sizes of Ag nanowires that had been extracted from *D. magna* hemolymph. The analysis of the hemolymph required only dilution and bath sonication, forgoing the need for a total tissue digestion. This study also is a rare demonstration of how spICP-MS can be used to characterize different NP morphologies, as when the diameter of the tube is known, the length of the nanowire can be calculated from the mass response signal of the NP event [58]. Other studies have shown the capability of spICP-MS to detect metal wear particles in hip aspirates from metal-on-metal arthroplasty [107] and serum samples [109]. spICP-MS may also have the

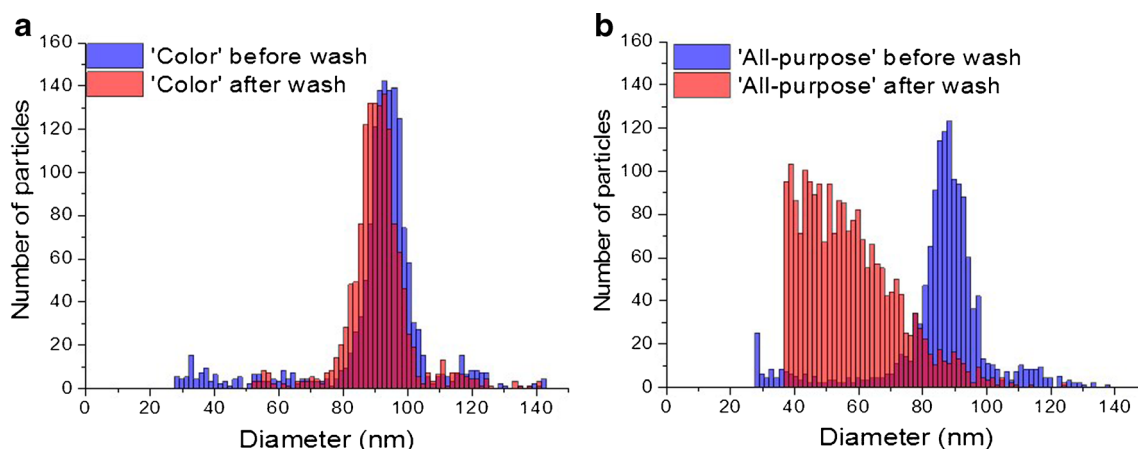


Fig. 4 Size distribution of 100 nm silver nanoparticles in different dry power laundry detergents before and after wash cycles. **(a)** Silver nanoparticle size distributions before and after wash cycle in color

detergent. **(b)** Silver nanoparticle size distributions before and after wash cycle in all-purpose detergent. Adapted from Mitrano et al. [134] Copyright (2015) American Chemical Society

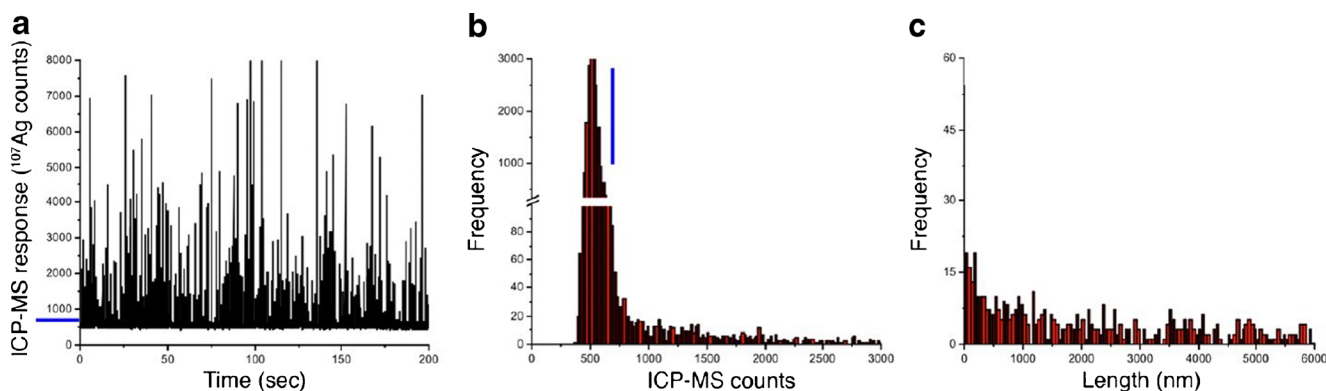


Fig. 5 Silver nanowire uptake into *D. magna* hemolymph. (A) Raw signal from Ag NWs. (B) Frequency distribution of Ag NW data, showing the intensity cut-off used to separate NP signal from dissolved.

(C) Length distribution of Ag NWs calculated from count intensity. Adapted from Scanlan et al. Copyright (2013) American Chemical Society

potential to be used in highly selective immunoassay, as NPs can be functionalized with a number of different biomarkers, and the sensitivity of spICP-MS can be exploited to detect these bioconjugated particles [138–140].

Industrial materials characterization

Nanomaterials used in industrial processes also possess a high likelihood for release into the environment. Current estimates place the production of certain metal oxide nanoparticles (zinc oxide, titanium dioxide, silica) in the tens of thousands of tons per year [141]. These materials are used in a variety of applications from pigments and coatings, filler materials in composites, and abrasive particles used in planarization processes for microchip fabrication [119]. In these industries, the size of the NPs has a significant effect on their desired properties. As such, having a high-throughput technique capable of assessing particle size and aggregation state is an attractive prospect for these applications. There are many techniques currently available, both ensemble and single particle, which are capable of sizing these particles, but many lack the specificity and sensitivity of spICP-MS.

A recent review by Speed et al. [119] compares different sizing techniques for nanoparticles used in chemical-mechanical polishing slurries, namely CeO_2 , Al_2O_3 , and two different types of SiO_2 NPs (alkaline and fumed). It should be noted that the colloidal silica size could not be determined by spICP-MS because of its small size and the high background. This is a limitation of ICP-Q-MS, which lacks the requisite resolution to differentiate atomic species from molecular species that possess the same nominal mass. This is particularly prevalent from elements such as $^{56}\text{Fe}^+$ and $^{28}\text{Si}^+$, the detection of which are impeded by prevalent concentrations for $^{56}\text{ArO}^+$ and $^{28}\text{N}_2^+$, respectively [142]. Other masses of these elements may be used in some cases, such as ^{57}Fe and ^{30}Si , but these isotopes are present at much lower abundances, which limit their size detection limit [92, 143]. The advent of microsecond

dwelt times may allow for the detection of the most abundant isotope, as the constant interference from the molecular species will be reduced in proportion to dwell time [144]. Alternatively, an ICP-MS with a reaction cell could be used to reduce or eliminate spectral overlaps from many polyatomic ions (such as ArO^+).

Nanoparticle sizes measured by different techniques are compared in Fig. 6, where it can be shown that some techniques such as dynamic light scattering (DLS) and nanotracking analysis (NTA) may overestimate particle sizes (likely due to light scattering principles), while sizes measured by electron microscopy are lower sizes, smaller due to its ability to accurately discern the primary particle sizes. The data collected from spICP-MS reside within these two size regimes. CeO_2 and Al_2O_3 particle sizes measured by spICP-MS were closer to the values provided by SEM and TEM. Fumed silica NP sizes measured by spICP-MS were closer to that reported by light scattering techniques. This is likely due to the prevalent molecular interferences that inhibit the

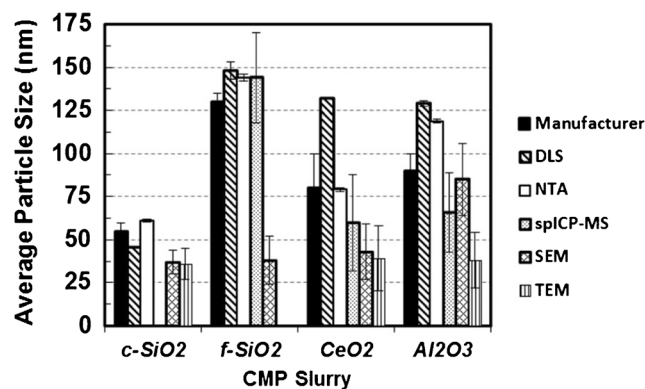


Fig. 6 Comparison of the average particle sizes determined by Speed et al. [119] various CMP slurries (colloidal SiO_2 , fumed SiO_2 , CeO_2 , and Al_2O_3) using different particle sizing techniques with values reported by the slurry manufacturer. Reproduced by permission of The Royal Society of Chemistry

detection of silicon ions resulting in undetectable signals for small particles.

Figure 6 is also illustrative of the current status of the accuracy and comparability of NP sizing of complex materials using multiple methodologies. Each technique tends to give a different result for mean size and distribution width. In the case of monodisperse standards, TEM/SEM is the technique by which all other approaches are compared. However, as is illustrated for the CMP example, if aggregation or complex morphology is involved, the “correct” particle size may be difficult to define even for TEM/SEM.

Remaining challenges and future directions

A number of challenges remain for spICP-MS to obtain consistently accurate average NP size, NP size distributions, and NP number concentrations as indicated by the results of a round robin study [38]. A number of key issues require further study.

Challenges for spICP-MS development can be particularly difficult to overcome if standard reference materials with very carefully determined NP sizes, NP distributions, and NP number concentrations are not available, such as those provided by the National Institute of Standards and Technology (NIST) (NIST RM 8011, 8012, 8013). Many of the commercially available NP suspensions are not characterized to the extent of the NIST materials. For example, NP size distributions are often based on scanning electron microscopy (SEM) or transmission electron microscopy (TEM) measurement of just 100 or so NP. Furthermore, the density and shape of the NPs must be known in order to relate spICP-MS signal, which depends on the total mass of analyte in the NP, to the NP diameter. This is true for both the analyte NP and the standard NP used for calibration. In spICP-MS publications to date, the density of the nanoparticle is typically assumed to be independent of particle size and equal to the density of the bulk material. However, this may not be true. By comparing the size of NPs determined by spICP-MS and other size fractionation techniques, such as flow and sedimentation-FFF, it may be possible to determine the density (porosity) of the NPs.

Despite showing considerable promise as a sensitive and selective technique for nanomaterial characterization, the size detection limit for most elements is still too high (>10 nm) for most nanomaterials that are generated for commercial purposes [92]. Some ICP-MS instruments, including ICP-Sector Field MS (ICP-SFMS) instruments used at a resolving power of 300 and at least one commercial quadrupole based ICP-MS, can provide sensitivities greater than 1 million counts s^{-1} ppb^{-1} from analytes in solution (up to 10× higher than most quadrupole instruments). As a result of the higher sensitivity, these instruments can detect Au NPs as small as 8 nm [51]. Special high sensitivity interfaces, with specially shaped

sampler and skimmer cones and additional pumping can provide further enhanced sensitivities. Although for reasons not fully understood, the highest sensitivities (up to about 50 million counts s^{-1} ppb^{-1}) [145] have only been obtained when a desolvation system was used.

If the spICP-MS measurements are based on one element, it is impossible to distinguish between two different particles and a particle that contains two or more elements. ICP-TOFMS can measure multiple elements simultaneously so that major elements can be measured and the chemical composition determined on a particle-by-particle basis if the particle has a large enough mass of each element and if the instrument can store all of the measurement without prior averaging. Multi-collector-inductively coupled plasma-mass spectrometry (MC-ICP-MS) is capable of measuring multiple isotopes (over a narrow range of masses) simultaneously and has been used to determine isotope ratios from individual nanoparticles [146]. Fast-scanning quadrupole MS may allow measurement of two isotopes in a particle. Combinations of spICP-MS and separation techniques, such as field flow fractionation (FFF) or capillary electrophoresis, may also be able to answer the question if an impurity is in the NPs or if the impurity is due to small numbers of nanoparticles of another element. Development of multi-element spICP-MS will be a significant advancement in its application to more complex NPs.

spICP-MS may be useful in investigating nanoparticle aggregation, particularly if the size or total mass of the individual nanoparticles is known. However, because colloids are dynamic, changes in aggregation due to the sample preparation (often including sonication), sample storage, and nebulization processes must be considered. Furthermore, the degree to which loose aggregates are maintained during spICP-MS analysis must be quantified.

Accurate measurement of NP number concentrations may be possible by spICP-MS and would be one of its most powerful attributes. The transport efficiency of NP from the sample vessel to the nebulizer and then through the spray chamber into the plasma must be known or determined in order to compute the number concentrations of the sample. In order to use transport efficiency to make this calculation, any loss of nanoparticles during transport from the sample container to the plasma must be the same for the NP standards and the sample. The use of sample introduction systems with virtually 100 % transport efficiency could alleviate some of these potential problems.

The effect of the sample matrix on the ICP-MS sensitivities (counts/fg) from nanoparticles and solution needs further investigation. The sample matrix could affect either the transport efficiency, the sensitivity, or both. Matrix matching or internal standardization may provide a means to compensate for matrix effects. However, if both the transport efficiency and the sensitivity are affected by the matrix, a single internal

standard will not be sufficient. Questions even remain about whether or not ICP-MS sensitivities (counts/fg) are the same for NP as solutions (even when matrix-matched).

Although spICP-MS is able to quantify the signal from dissolved analyte, if that signal is too large, the minimum detectable nanoparticle size will increase [52, 51, 58]. This is a particular issue for NPs with a tendency to dissolve in the environment such as silver, zinc oxide, and copper oxide nanoparticles. In addition, as the signal of dissolved analyte becomes larger, noise of that signal could result in misidentification of signal fluctuations as signals from nanoparticles. The simplest solution is to select a conservative background cut-off ($>5\sigma$ above the average) that attempts to ensure that any signal detected above this threshold originates from an NP event [46, 113]. Most recently, this method was used to accurately detect copper containing sediment particles from soil extracts that had been spiked with copper oxide nanoparticles [147]. Though utilizing a conservative 7σ threshold cut-off for the background, this research demonstrated a low presence of NNPs with a detectable copper signal, concluding the nanoparticulate signal registered must originate from copper ENPs or copper NPs and ions adsorbed to soil particulate. However, this will also increase the minimum size nanoparticle that can be accurately detected.

spICP-MS seems to be ideally suited to investigate NP biological uptake, but there are still facets of the technique that need to be addressed. It is still unknown to what degree the biological matrix affects the signal produced from a NP, and if this change is consistent with that of corresponding dissolved analyte. Additionally, extraction methods for NPs from biological tissues are still underdeveloped, as different tissues and different NPs may require more sophisticated means of extraction than those described here. Despite these challenges, there are many questions that spICP-MS is ideally suited to address, such as the transformation processes in biological tissues, tracking the uptake of NPs through plant translocation, and potentially the study for the formation of protein coronas on nanoparticles, which are shown to significantly impact their potential toxicity.

The continued production of nanomaterials necessitates the ongoing development of sensitive and specific techniques capable of monitoring nanomaterial release and transformation at environmentally relevant concentrations. Though there are many questions still remaining regarding the performance of spICP-MS, it has quickly been established as a premiere technique for the element specific analysis of nanomaterials in complex matrices. Efforts made to improve various aspects of the technique, such as sensitivity and data processing, will help considerably in broadening the number of materials and matrices that are capable of being assessed for nanomaterial risk.

Acknowledgments The authors acknowledge graduate student support from the National Science Foundation (CBET-1336168, -1512695), the

Environmental Protection Agency (RD83558001). Postdoctoral support comes from the Center for the Environmental Implications of Nanotechnology.

Compliance with Ethical Standards

Conflicts of interest The authors declare that they have no conflict of interest.

References

1. Degueldre C, Favarger PY. Colloid analysis by single particle inductively coupled plasma-mass spectroscopy: a feasibility study. *Colloids Surf A Physicochem Eng Aspects*. 2003;217(1/3):137–42.
2. Mattson S. The laws of soil colloidal behavior: I. *Soil Sci*. 1929;28(3):179–220.
3. Myers HE. Physicochemical reactions between organic and inorganic soil colloids as related to aggregate formation. *Soil Sci*. 1937;44(5):331–60.
4. Goldberg ED Marine geochemistry I. Chemical scavengers of the sea. *J Geology*. 1954 249–265.
5. Krauskopf KB. Factors controlling the concentrations of thirteen rare metals in sea-water. *Geochim Cosmochim Acta*. 1956;9(1):1–B32.
6. Sillen LG The physical chemistry of sea water. *Oceanography*. American Association for the Advancement of Science, Washington, DC; 1961. pp. 549–581.
7. Sneddon J. Collection and atomic spectroscopic measurement of metal compounds in the atmosphere: a review. *Talanta*. 1983;30(9):631–48.
8. Edwards HW. Direct determination of silver in air by atomic absorption spectrometry. *Anal Chem*. 1969;41(10):1172–5.
9. Crider WL. Spectrothermal emission aerosol particle analyzer (Seapa). *Rev Sci Instrum*. 1968;39(2):212–5.
10. Lorenz G. Method of and apparatus for use in measuring the particle size distribution and/or the concentration of particles in suspension in a gaseous dispersing medium. Google Patents; 1974.
11. Kawaguchi H, Fukasawa N, Mizuike A. Investigation of airborne particles by inductively coupled plasma emission spectrometry calibrated with monodisperse aerosols. *Spectrochim Acta, Part B*. 1986;41(12):1277–86.
12. Bochert U, Dannecker W. On-line aerosol analysis by atomic emission spectroscopy. *J Aerosol Sci*. 1989;20(8):1525–8.
13. Kaneco S, Nomizu T, Tanaka T, Mizutani N, Kawaguchi H. Optimization of operating conditions in individual airborne particle analysis by inductively coupled plasma mass spectrometry. *Anal Sci*. 1995;11(5):835–40.
14. Nomizu T, Hayashi H, Hoshino N, Tanaka T, Kawaguchi H, Kitagawa K, et al. Determination of zinc in individual airborne particles by inductively coupled plasma mass spectrometry with digital signal processing. *J Anal At Spectrom*. 2002;17(6):592–5.
15. Nomizu T, Kaneco S, Tanaka T, Yamamoto T, Kawaguchi H. Determination of femtogram amounts of zinc and lead in individual airborne particles by inductively coupled plasma mass spectrometry with direct air-sample introduction. *Anal Sci*. 1993;9(6):843–6.
16. Nomizu T, Nakashima H, Hotta Y, Tanaka T, Kawaguchi H. Simultaneous measurement of the elemental content and size of airborne particles by inductively coupled plasma emission spectrometry combined with the laser light-scattering method. *Anal Sci*. 1992;8(4):527–31.

17. Noble CA, Prather KA. Real-time single particle mass spectrometry: a historical review of a quarter century of the chemical analysis of aerosols. *Mass Spectrom Rev.* 2000;19(4):248–74.
18. McCarthy JF, Zachara JM. Subsurface transport of contaminants. *Environ Sci Technol.* 1989;23(5):496–502.
19. Penrose WR, Polzer WL, Essington EH, Nelson DM, Orlandini KA. Mobility of plutonium and americium through a shallow aquifer in a semiarid region. *Environ Sci Technol.* 1990;24(2):228–34.
20. Smith P, Degueldre C. Colloid-facilitated transport of radionuclides through fractured media. *J Contam Hydrol.* 1993;13(1):143–66.
21. McCarthy J, Degueldre C. Characterization of environmental particles. Chelsea, MI: Lewis Publishers; 1993.
22. Degueldre C, Favarger PY. Thorium colloid analysis by single particle inductively coupled plasma-mass spectrometry. *Talanta.* 2004;62(5):1051–4.
23. Degueldre C, Favarger P-Y, Bitea C. Zirconia colloid analysis by single particle inductively coupled plasma-mass spectrometry. *Anal Chim Acta.* 2004;518(1):137–42.
24. Degueldre C, Favarger P-Y, Rosse R, Wold S. Uranium colloid analysis by single particle inductively coupled plasma-mass spectrometry. *Talanta.* 2006;68(3):623–8.
25. Degueldre C, Favarger P-Y, Wold S. Gold colloid analysis by inductively coupled plasma-mass spectrometry in a single particle mode. *Anal Chim Acta.* 2006;555(2):263–8.
26. Laborda F, Jimenez-Lamana J, Bolea E, Castillo JR. Selective identification, characterization and determination of dissolved silver(i) and silver nanoparticles based on single particle detection by inductively coupled plasma mass spectrometry. *J Anal At Spectrom.* 2011;26(7):1362–71.
27. Hasselov M, Readman J, Ranville J, Tiede K. Nanoparticle analysis and characterization methodologies in environmental risk assessment of engineered nanoparticles. *Ecotoxicology.* 2008;17(5):344–61.
28. Montano MD, Lowry GV, von der Kammer F, Blue J, Ranville JF. Current status and future direction for examining engineered nanoparticles in natural systems. *Environ Chem.* 2014;11:351–66. doi:10.1071/EN14037.
29. Laborda F, Bolea E, Cepriá G, Gómez MT, Jiménez MS, Pérez-Arantegui J, et al. Detection, characterization, and quantification of inorganic engineered nanomaterials: a review of techniques and methodological approaches for the analysis of complex samples. *Anal Chim Acta.* 2016;904:10–32.
30. Laborda F, Bolea E, Jimenez-Lamana J. Single particle inductively coupled plasma mass spectrometry: a powerful tool for nanoanalysis. *Anal Chem.* 2013;86(5):2270–8.
31. Olesik JW, Gray PJ. Considerations for measurement of individual nanoparticles or microparticles by ICP-MS: determination of the number of particles and the analyte mass in each particle. *J Anal At Spectrom.* 2012;27(7):1143–55.
32. Lee W-W, Chan W-T. Calibration of single-particle inductively coupled plasma-mass spectrometry (SP-ICP-MS). *J Anal At Spectrom.* 2015;30:1245–54. doi:10.1039/C4JA00408F.
33. French JB, Etkin B, Jong R. Monodisperse dried microparticulate injector for analytical instrumentation. *Anal Chem.* 1994;66(5):685–91.
34. Olesik JW, Hobbs SE. Monodisperse dried microparticulate injector: a new tool for studying fundamental processes in inductively coupled plasmas. *Anal Chem.* 1994;66(20):3371–8.
35. Garcia CC, Murtazin A, Groh S, Horvatic V, Niemax K. Characterization of single Au and SiO₂ nano- and microparticles by ICP-OES using monodisperse droplets of standard solutions for calibration. *J Anal At Spectrom.* 2010;25(5):645–53.
36. Gschwind S, Flamigni L, Koch J, Borovinskaya O, Groh S, Niemax K, et al. Capabilities of inductively coupled plasma mass spectrometry for the detection of nanoparticles carried by monodisperse microdroplets. *J Anal At Spectrom.* 2011;26(6):1166–7411.
37. Borovinskaya O, Gschwind S, Hattendorf B, Tanner M, Günther D. Simultaneous mass quantification of nanoparticles of different composition in a mixture by microdroplet generator-ICPTOFMS. *Anal Chem.* 2014;86(16):8142–48. doi:10.1021/ac501150c.
38. Montoro Bustos AR, Petersen EJ, Possolo A, Winchester MR. Post hoc interlaboratory comparison of single particle ICP-MS size measurements of NIST gold nanoparticle reference materials. *Anal Chem.* 2015;87(17):8809–17.
39. Pace HE, Rogers NJ, Jarolimek C, Coleman VA, Higgins CP, Ranville JF. Determining transport efficiency for the purpose of counting and sizing nanoparticles via single particle inductively coupled plasma mass spectrometry. *Anal Chem.* 2011;83(24):9361–9.
40. Willis JB. Atomization problems in atomic absorption spectroscopy—I. A study of the operation of a typical nebulizer, spray chamber, and burner system. *Spectrochim Acta, Part A.* 1967;23(4):811–30.
41. Smith DD, Browner RF. Measurement of aerosol transport efficiency in atomic spectrometry. *Anal Chem.* 1982;54(3):533–7.
42. Tuoriniemi J, Cornelis G, Hasselöv M. Improving the accuracy of single particle ICPMS for measurement of size distributions and number concentrations of nanoparticles by determining analyte partitioning during nebulisation. *J Anal At Spectrom.* 2014;29(4):743–52.
43. Verwey EJW, Overbeek JTG, Overbeek JTG. Theory of the stability of lyophobic colloids. Courier Corporation 1999.
44. Derjaguin B, Landau L. Theory of the stability of strongly charged lyophobic sols and of the adhesion of strongly charged particles in solutions of electrolytes. *Prog Surf Sci.* 1993;43(1/4):30–59.
45. Falabella JB, Cho TJ, Ripple DC, Hackley VA, Tarlov MJ. Characterization of gold nanoparticles modified with single-stranded DNA using analytical ultracentrifugation and dynamic light scattering. *Langmuir.* 2010;26(15):12740–7.
46. Reed RB, Goodwin DG, Marsh KL, Capracotta SS, Higgins CP, Fairbrother DH, et al. Detection of single walled carbon nanotubes by monitoring embedded metals. *Environ Sci.* 2013;15(1):204–13.
47. Pace HE, Rogers NJ, Jarolimek C, Coleman VA, Gray EP, Higgins CP, et al. Single particle inductively coupled plasma-mass spectrometry: a performance evaluation and method comparison in the determination of nanoparticle size. *Environ Sci Technol.* 2012;46(22):12272–80. doi:10.1021/es301787d.
48. Mitrano DM, Leshner EK, Bednar A, Monserud J, Higgins CP, Ranville JF. Detecting nanoparticulate silver using single-particle inductively coupled plasma-mass spectrometry. *Environ Toxicol Chem.* 2012;31(1):115–21.
49. Hineman A, Stephan C. Effect of dwell time on single particle inductively coupled plasma mass spectrometry data acquisition quality. *J Anal At Spectrom.* 2014;29:1252–57. doi:10.1039/C4JA00097H.
50. Montaña MD, Badieli HR, Bazargan S, Ranville JF. Improvements in the detection and characterization of engineered nanoparticles using spICP-MS with microsecond dwell times. *Environ Sci Nano.* 2014;1:338–46. doi:10.1039/C4EN00058G.
51. Tuoriniemi J, Cornelis G, Hasselöv M. A new peak recognition algorithm for detection of ultra-small nano-particles by single particle ICP-MS using rapid time resolved data acquisition on a sector-field mass spectrometer. *J Anal At Spectrom.* 2015;30(8):1723–9.
52. Liu J, Murphy KE, MacCuspie RI, Winchester MR. Capabilities of single particle inductively coupled plasma mass spectrometry for the size measurement of nanoparticles: a case study on gold

- nanoparticles. *Anal Chem.* 2014;86(7):3405–14. doi:10.1021/ac403775a.
53. Hadioui M, Peyrot C, Wilkinson KJ. Improvements to Single Particle ICPMS by the online coupling of ion exchange resins. *Anal Chem.* 2014;86(10):4668–74. doi:10.1021/ac5004932.
 54. Montoro Bustos A, Purushotham K, Vladár A, Murphy K, Winchester M Matrix effects and validation of single particle ICP-MS for measuring nanoparticle size and size distribution. *Proceedings of the Winter Conference on Plasma Spectrochemistry*; Tucson, AZ. 2016.
 55. El Hadri H, Petersen EJ, Winchester MR. Impact of and correction for instrument sensitivity drift on nanoparticle size measurements by single-particle ICP-MS. *Anal Bioanal Chem* 2016; 1–10.
 56. Cornelis G, Rauch S Drift correction of the dissolved signal in single particle ICPMS. *Anal Bioanal Chem.* 2016; 1–13
 57. Cornelis G, Hassellöv M. A signal deconvolution method to discriminate smaller nanoparticles in single particle ICP-MS. *J Anal At Spectrom.* 2014;29(1):134–44.
 58. Scanlan LD, Reed RB, Loguinov AV, Antczak P, Tagmount A, Aloni S. Silver nanowire exposure results in internalization and toxicity to *Daphnia magna*. *ACS Nano.* 2013;7(12):10681–94. doi:10.1021/nn4034103.
 59. Masalov V, Sukhinina N, Kudrenko E, Emelchenko G. Mechanism of formation and nanostructure of Stöber silica particles. *Nanotechnology.* 2011;22(27):275718.
 60. Rahman IA, Vejayakumaran P, Sipaut CS, Ismail J, Chee CK. Size-dependent physicochemical and optical properties of silica nanoparticles. *Mat Chem Phys.* 2009;114(1):328–32.
 61. Houk R. Mass spectrometry of inductively coupled plasmas. *Anal Chem.* 1986;58(1):97A–105A.
 62. Houk RS, Fassel VA, Flesch GD, Svec HJ, Gray AL, Taylor CE. Inductively coupled argon plasma as an ion source for mass spectrometric determination of trace elements. *Anal Chem.* 1980;52(14):2283–9.
 63. Date AR, Gray AL. Development progress in plasma source mass spectrometry. *Analyst (Cambridge, U K).* 1983;108(1283):159–65.
 64. Hieftje GM, Vickers GH. Developments in plasma source/mass spectrometry. *Anal Chim Acta.* 1989;216:1–24.
 65. Nelms SM, editor. *Inductively Coupled Plasma Mass Spectrometry Handbook.* Oxford: Blackwell Publishing Ltd.; 2005.
 66. Olesik JW. Investigating the fate of individual sample droplets in inductively coupled plasmas. *Appl Spectrosc.* 1997;51(5):158A.
 67. Olesik JW, Bates LC. Characterization of aerosols produced by pneumatic nebulizers for inductively coupled plasma sample introduction: effect of liquid and gas flow rates on volume based drop size distributions. *Spectrochim Acta, Part B.* 1995;50(4/7): 285–303.
 68. Olesik JW, Stewart II, Hartshorne JA, Hensman CE. Sensitivity and matrix effects in ICP-MS: aerosol processing, ion production and ion transport. In: Tanner SD, Holland G, editors. *Plasma source mass spectrometry: new developments and applications*, pp 1–19. Cambridge: Royal Society of Chemistry; 1999.
 69. Olesik JW *Inductively Coupled Plasma Mass Spectrometers.* In: Holland H, Turekian KK, (Eds) *Treatise on Geochemistry*, 2nd ed. Elsevier; 2014. pp 309–336.
 70. Todoli JL, Mermert JM. Sample introduction systems for the analysis of liquid microsamples by ICP-AES and ICP-MS. *Spectrochim Acta, Part B.* 2006;61(3):239–83.
 71. Olesik JW, Hensman C, Rabb S, Rago D. Sample introduction, plasma-sample interactions, ion transport, and ion–molecule reactions: fundamental understanding and practical improvements in ICP-MS. In: Tanner SD, Holland G, (Eds) *Plasma source mass spectrometry: the new millenium*, pp. 3–17; Royal Society of Chemistry: Cambridge; 2001.
 72. S-i M, Groombridge AS, S-i F, Minoda A, Takatsu A, Hioki A, et al. Highly efficient single-cell analysis of microbial cells by time-resolved inductively coupled plasma mass spectrometry. *J Anal At Spectrom.* 2014;29(9):1598–606.
 73. Gschwind S, Hagendorfer H, Frick DA, Günther D. Mass quantification of nanoparticles by single droplet calibration using inductively coupled plasma mass spectrometry. *Anal Chem.* 2013;85(12):5875–83.
 74. Borovinskaya O, Hattendorf B, Tanner M, Gschwind S, Günther D. A prototype of a new inductively coupled plasma time-of-flight mass spectrometer providing temporally resolved, multi-element detection of short signals generated by single particles and droplets. *J Anal At Spectrom.* 2013;28(2):226–33.
 75. Koch J, Flamigni L, Gschwind S, Allner S, Longereich H, Gunther D. Accelerated evaporation of microdroplets at ambient conditions for the on-line analysis of nanoparticles by inductively-coupled plasma mass spectrometry. *J Anal At Spectrom.* 2013;28(11): 1707–17.
 76. Verboket PE, Borovinskaya O, Meyer N, Günther D, Dittrich PS. A new microfluidics-based droplet dispenser for ICPMS. *Anal Chem.* 2014;86(12):6012–8.
 77. Orlandini V, Niessen JO, Schaper JN, Petersen JH, Bings NH. Development and characterization of a thermal inkjet-based aerosol generator for micro-volume sample introduction in analytical atomic spectrometry. *J Anal At Spectrom.* 2011;26(9):1781–9.
 78. Dettman JR. Experimental measurements and modeling to understand sensitivity and plasma sample loading in inductively coupled plasma optical emission spectrometry. Thesis. The Ohio State University 2011.
 79. Hobbs SE, Olesik JW. Inductively coupled plasma mass spectrometry signal fluctuations due to individual aerosol droplets and vaporizing particles. *Anal Chem.* 1992;64(3):274–83.
 80. Groh S, Garcia CC, Murtazin A, Horvatic V, Niemax K. Local effects of atomizing analyte droplets on the plasma parameters of the inductively coupled plasma. *Spectrochim Acta, Part B.* 2009;64(3):247–54.
 81. Ho K-S, Lee W-W, Chan W-T. Effects of ionization potential of an element and boiling point of the corresponding oxide on the sensitivity of ICP-MS. *J Anal At Spectrom.* 2015;30:2066–73.
 82. Ho KS, Lui KO, Lee KH, Chan WT. Considerations of particle vaporization and analyte diffusion in single-particle inductively coupled plasma-mass spectrometry. *Spectrochim Acta, Part B.* 2013;89:30–9.
 83. Olesik JW, Dziewatkoski MP. Time-resolved measurements of individual ion cloud signals to investigate space-charge effects in plasma mass spectrometry. *J Am Soc Mass Spectrom.* 1996;7(4): 362–7.
 84. Olesik JW, Kinzer JA, McGowan GJ. Observation of atom and ion clouds produced from single droplets of sample in inductively coupled plasmas by optical emission and laser-induced fluorescence imaging. *Appl Spectrosc.* 1997;51(5):607–16.
 85. Dziewatkoski MP, Daniels LB, Olesik JW. Time-resolved inductively coupled plasma mass spectrometry measurements with individual, monodisperse drop sample introduction. *Anal Chem.* 1996;68(7):1101–9.
 86. Lindner H, Murtazin A, Groh S, Niemax K, Bogaerts A. Simulation and experimental studies on plasma temperature, flow velocity, and injector diameter effects for an inductively coupled plasma. *Anal Chem.* 2011;83(24):9260–6.
 87. Aghaei M, Bogaerts A. Particle transport through an inductively coupled plasma torch: elemental droplet evaporation. *J Anal At Spectrom.* 2016;31:631–641. doi:10.1039/C5JA00162E.
 88. Aghaei M, Flamigni L, Lindner H, Günther D, Bogaerts A. Occurrence of gas flow rotational motion inside the ICP torch: a computational and experimental study. *J Anal At Spectrom.* 2014;29(2):249–61.

89. Borovinskaya O, Aghaei M, Flamigni L, Hattendorf B, Tanner M, Bogaerts A, et al. Diffusion-and velocity-driven spatial separation of analytes from single droplets entering an ICP off-axis. *J Anal At Spectrom.* 2014;29(2):262–71.
90. Montaña MD Studies into the detection, characterization, and behavior of naturally occurring and engineered inorganic nanoparticles. Thesis. The Colorado School of Mines 2014.
91. Peters R, Herrera-Rivera Z, Undas A, van der Lee M, Marvin H, Bouwmeester H, et al. Single particle ICP-MS combined with a data evaluation tool as a routine technique for the analysis of nanoparticles in complex matrices. *J Anal At Spectrom.* 2015;30(6):1274–85.
92. Lee S, Bi X, Reed RB, Ranville JF, Herckes P, Westerhoff P. Nanoparticle size detection limits by single particle ICP-MS for 40 elements. *Environ Sci Technol.* 2014;48(17):10291–300.
93. Stephan C Analysis of iron nanoparticles in organic solvents used in the semiconductor industry using single particle ICP-MS in reaction mode 2015. Report no.: Perkin Elmer Application Note 012407A_01. 2015.
94. Stewart II, Hensman CE, Olesik JW. Influence of gas sampling on analyte transport within the ICP and ion sampling for ICP-MS studied using individual, isolated sample droplets. *Appl Spectrosc.* 2000;54(2):164–74.
95. Douglas DJ, French JB. Gas dynamics of the inductively coupled plasma mass spectrometry interface. *J Anal At Spectrom.* 1988;3(6):743–7.
96. Olivares JA, Houk RS. Ion sampling for inductively coupled plasma mass spectrometry. *Anal Chem.* 1985;57(13):2674–9.
97. Tanner SD. Space charge in ICP-MS: calculation and implications. *Spectrochi Acta Part B.* 1992;47(6):809–23.
98. Tan SH, Horlick G. Matrix-effect observations in inductively coupled plasma mass spectrometry. *J Anal At Spectrom.* 1987;2(8):745–63.
99. Strenge I, Engelhard C. Capabilities of fast data acquisition with microsecond time resolution in inductively coupled plasma mass spectrometry and identification of signal artifacts from millisecond dwell times during detection of single gold nanoparticles. *J Anal At Spectrom.* 2016;31(1):135–44.
100. Miyashita S, Fujii S, Takatsu A, Inagaki K Evaluation of transport efficiency of nanoparticles through a total consumption sample introduction system in single particle ICP-MS. Proceedings of the Winter Conference on Plasma Spectrochemistry; Tucson, AZ 2016.
101. Yau MHP, Chan W-T. A novel detection scheme of trace elements using ICP-MS. *J Anal At Spectrom.* 2005;20(11):1197–202.
102. Stephan C, Hineman A. Analysis of NIST gold nanoparticles reference materials using the NexION 300 ICP-MS in single particle mode. Application Note, Perkin Elmer, Inc. 2012.
103. Hadioui M, Wilkinson K, Stephan C. Assessing the fate of silver nanoparticles in surface water using single particle ICP-MS. A Perkin Elmer Application note.
104. Sannac S. Single particle analysis of nanomaterials using the Agilent 7900 ICP-MS. An Agilent Application Note.
105. Kutscher D, Wills J, McSheehy Ducos S. Nanoparticle characterization via single particle inductively coupled plasma-mass spectrometry (spICP-MS) using a dedicated plug-in for Qtegra ISDS software. ThermoScientific Technical Note.43279.
106. Loeschner K, Navratilova J, Købler C, Mølhav K, Wagner S, Kammer F, et al. Detection and characterization of silver nanoparticles in chicken meat by asymmetric flow field flow fractionation with detection by conventional or single particle ICP-MS. *Anal Bioanal Chem.* 2013;405(25):8185–95.
107. Loeschner K, Harrington CF, Kearney J-L, Langton DJ, Larsen EH. Feasibility of asymmetric flow field-flow fractionation coupled to ICP-MS for the characterization of wear metal particles and metalloproteins in biofluids from hip replacement patients. *Anal Bioanal Chem.* 2015;407(16):4541–54.
108. Kim ST, Kim HK, Han SH, Jung EC, Lee S. Determination of size distribution of colloidal TiO₂ nanoparticles using sedimentation field-flow fractionation combined with single particle mode of inductively coupled plasma-mass spectrometry. *Microchem J.* 2013;110:636–42.
109. Roman M, Rigo C, Castillo-Michel H, Munivrana I, Vindigni V, Mičetić I. Hydrodynamic chromatography coupled to single-particle ICP-MS for the simultaneous characterization of AgNPs and determination of dissolved Ag in plasma and blood of burn patients. *Anal Bioanal Chem* 1–16 2015.
110. Proulx K, Wilkinson KJ. Separation, detection, and characterisation of engineered nanoparticles in natural waters using hydrodynamic chromatography and multi-method detection (light scattering, analytical ultracentrifugation, and single particle ICP-MS). *Environ Chem.* 2014;11(4):392–401.
111. Hadioui M, Merdzan V, Wilkinson KJ. Detection and characterization of ZnO nanoparticles in surface and waste waters using single particle ICPMS. *Environ Sci Technol.* 2015;49(10):6141–8.
112. Mitrano D, Ranville J, Bednar A, Kazor K, Hering A, Higgins C. Tracking dissolution of silver nanoparticles at environmentally relevant concentrations in laboratory, natural, and processed waters using single particle ICP-MS (spICP-MS). *Environ Sci: Nano.* 2014;1(3):248–59.
113. Reed RB, Higgins CP, Westerhoff P, Tadjiki S, Ranville JF. Overcoming challenges in analysis of polydisperse metal-containing nanoparticles by single particle inductively coupled plasma mass spectrometry. *J Anal At Spectrom.* 2012;27(7):1093–100.
114. Tuoriniemi J, Cornelis G, Hassellöv M. Size discrimination and detection capabilities of single-particle ICPMS for environmental analysis of silver nanoparticles. *Anal Chem.* 2012;84(9):3965–72.
115. Gondikas AP, Fvd K, Reed RB, Wagner S, Ranville JF, Hofmann T. Release of TiO₂ nanoparticles from sunscreens into surface waters: a one-year survey at the old Danube recreational lake. *Environ Sci Technol.* 2014;48(10):5415–22.
116. Roco MC, Mirkin CA, Hersam MC. Nanotechnology research directions for societal needs in 2020: summary of international study. *J Nanoparticle Res.* 2011;13(3):897–919.
117. Roco MC, Mirkin CA, Hersam MC Nanotechnology research directions for societal needs in 2020: Retrospective and outlook. Springer 2011.
118. Kiser MA, Westerhoff P, Benn T, Wang Y, Pérez-Rivera J, Hristovski K. Titanium nanomaterial removal and release from wastewater treatment plants. *Environ Sci Technol.* 2009;43(17):6757–63.
119. Speed D, Westerhoff P, Sierra-Alvarez R, Draper R, Pantano P, Aravamudan S, et al. Physical, chemical, and in vitro toxicological characterization of nanoparticles in chemical mechanical planarization suspensions used in the semiconductor industry: towards environmental health and safety assessments. *Environ Sci: Nano.* 2015;2(3):227–44.
120. Christian P, Kammer F, Baalousha M, Hofmann T. Nanoparticles: structure, properties, preparation and behavior in environmental media. *Ecotoxicology.* 2008;17(5):326–43.
121. Kah M, Hofmann T. Nanopesticide research: current trends and future priorities. *Environ Int.* 2014;63:224–35.
122. Benn T, Cavanagh B, Hristovski K, Posner JD, Westerhoff P. The Release of Nanosilver from Consumer Products Used in the Home Supplemental data file available online for this article. [All rights reserved. No part of this periodical may be reproduced or transmitted in any form or by any means, electronic or mechanical, including photocopying, recording, or any information storage and retrieval system, without permission in writing from the publisher.] *J Environ Qual.* 2010;39(6):1875–82.

123. Benn TM, Westerhoff P. Nanoparticle silver released into water from commercially available sock fabrics. *Environ Sci Technol*. 2008;42(11):4133–239.
124. Donovan AR, Adams CD, Ma Y, Stephan C, Eichholz T, Shi H. Single particle ICP-MS characterization of titanium dioxide, silver, and gold nanoparticles during drinking water treatment. *Chemosphere*. 2016;144:148–53.
125. Farkas J, Peter H, Christian P, Gallego Urrea JA, Hassellöv M, Tuoriniemi J, et al. Characterization of the effluent from a nanosilver producing washing machine. *Environ Int*. 2011;37(6):1057–62.
126. Peters RJ, Rivera ZH, van Bommel G, Marvin HJ, Weigel S, Bouwmeester H. Development and validation of single particle ICP-MS for sizing and quantitative determination of nano-silver in chicken meat. *Anal Bioanal Chem*. 2014;406(16):3875–85.
127. Linsinger TP, Peters R, Weigel S. International interlaboratory study for sizing and quantification of Ag nanoparticles in food simulants by single-particle ICPMS. *Anal Bioanal Chem*. 2014;406(16):3835–43.
128. Ramos K, Gómez-Gómez MM, Cámara C, Ramos L. Silver speciation and characterization of nanoparticles released from plastic food containers by single particle ICPMS. *Talanta*. 2016;151:83–90. doi:10.1016/j.talanta.2015.12.071.
129. Verleysen E, Van Doren E, Waegeneers N, De Temmerman P-J, Abi Daoud Francisco M, Mast J. TEM and SP-ICP-MS analysis of the release of silver nanoparticles from decoration of pastry. *J Agri Food Chem*. 2015;63(13):3570–8.
130. Szakal C, Roberts SM, Westerhoff P, Bartholomaeus A, Buck N, Illuminato I, et al. Measurement of nanomaterials in foods: integrative consideration of challenges and future prospects. *ACS Nano*. 2014;8(4):3128–35.
131. Singh G, Stephan C, Westerhoff P, Carlander D, Duncan TV. Measurement methods to detect, characterize, and quantify engineered nanomaterials in foods. *Comprehens Rev Food Sci Food Safety*. 2014;13(4):693–704.
132. António D, Cascio C, Jakšić Ž, Jurašin D, Lyons D, Nogueira A. Assessing silver nanoparticles behavior in artificial seawater by mean of AF4 and spICP-MS. *Marine Environ Res*; 2015.
133. Furtado L, Hoque M, Mitrano D, Ranville J, Cheever B, Frost P. The persistence and transformation of silver nanoparticles in littoral lake mesocosms monitored using various analytical techniques. *Environ Chem*; 2014.
134. Mitrano DM, Arroyo Rojas Dasilva Y, Nowack B. Effect of variations of washing solution chemistry on nanomaterial physico-chemical changes in the laundry cycle. *Environ Sci Technol*. 2015;49(16):9665–73.
135. Coleman JG, Kennedy AJ, Bednar AJ, Ranville JF, Laird JG, Harmon AR, et al. Comparing the effects of nanosilver size and coating variations on bioavailability, internalization, and elimination, using *Lumbriculus variegatus*. *Environ Toxicol Chem*. 2013;32(9):2069–77.
136. Gray EP, Coleman JG, Bednar AJ, Kennedy AJ, Ranville JF, Higgins CP. Extraction and analysis of silver and gold nanoparticles from biological tissues using single particle inductively coupled plasma mass spectrometry. *Environ Sci Technol*;2013.
137. Dan Y, Zhang W, Xue R, Ma X, Stephan C, Shi H. Characterization of gold nanoparticle uptake by tomato plants using enzymatic extraction followed by single-particle inductively coupled plasma-mass spectrometry analysis. *Environ Sci Technol*. 2015;49(5):3007–14.
138. Hu S, Liu R, Zhang S, Huang Z, Xing Z, Zhang X. A new strategy for highly sensitive immunoassay based on single-particle mode detection by inductively coupled plasma mass spectrometry. *J Am Soc Mass Spectrom*. 2009;20(6):1096–103.
139. Han G, Xing Z, Dong Y, Zhang S, Zhang X. One-step homogeneous DNA assay with single-nanoparticle detection. *Angew Chem Int Ed*. 2011;50(15):3462–5.
140. Zhang S, Han G, Xing Z, Zhang S, Zhang X. Multiplex DNA assay based on nanoparticle probes by single particle inductively coupled plasma mass spectrometry. *Anal Chem*. 2014;86(7):3541–7.
141. Nowack B, Bornhöft N, Ding Y, Riediker M, Jiménez AS, Sun T. The flows of engineered nanomaterials from production, use, and disposal to the environment. *The Handbook of Environmental Chemistry*. 2015;48:209–31.
142. Tanner SD, Baranov VI, Bandura DR. Reaction cells and collision cells for ICP-MS: a tutorial review. *Spectrochim Acta, Part B*. 2002;57(9):1361–452.
143. Leshner EK, Ranville JF, Honeyman BD. Analysis of pH dependent uranium(VI) sorption to nanoparticulate hematite by flow field-flow fractionation-inductively coupled plasma mass spectrometry. *Environ Sci Technol*. 2009;43(14):5403–9.
144. Montano MD, Majestic BJ, Jamting AK, Westerhoff P, Ranville JF. Methods for the detection and characterization of silica colloids by microsecond spICP-MS. *Anal Chem*. 2016;88(9):4733–41.
145. Zheng J. Evaluation of a new sector-field ICP-MS with Jet Interface for ultra-trace determination of Pu isotopes: from femtogram to attogram levels. *J Nucl Radiochem Sci*. 2015;15(1):7–13.
146. Yongyang S, Wei W, Zhiming L, Hu D, Guoqing Z, Jiang X, et al. Direct detection and isotope analysis of individual particles in suspension by single particle mode MC-ICP-MS for nuclear safety. *J Anal At Spectrom*. 2015;30(5):1184–90.
147. Navratilova J, Praetorius A, Gondikas A, Fabienke W, von der Kammer F, Hofmann T. Detection of engineered copper nanoparticles in soil using single particle ICP-MS. *Int J Environ Res Public Health*. 2015;12(12):15756–68.